National Library of Canada
Bibliothèque nationale du Canada

Canadian Theses Service
Service des thèses canadiennes

Ottawa, Canada
K1A 0N4

NOTICE

The quality of this microform is heavily dependent upon the quality of the original thesis submitted for microfilming. Every effort has been made to ensure the highest quality of reproduction possible.

If pages are missing, contact the university which granted the degree.

Some pages may have indistinct print especially if the original pages were typed with a poor typewriter ribbon or if the university sent us an inferior photocopy.

Reproduction in full or in part of this microform is governed by the Canadian Copyright Act, R.S.C. 1970, c. C-30, and subsequent amendments.

AVIS

La qualité de cette microforme dépend grandement de la qualité de la thèse soumise au microfilmage. Nous avons tout fait pour assurer une qualité supérieure de reproduction.

S'il manque des pages, veuillez communiquer avec l'université qui a conféré le grade.

La qualité d'impression de certaines pages peut laisser à désirer, surtout si les pages originales ont été dactylographiées à l'aide d'un ruban usé ou si l'université nous a fait parvenir une photocopie de qualité inférieure.

La reproduction, même partielle, de cette microforme est soumise à la Loi canadienne sur le droit d'auteur, SRC 1970, c. C-30, et ses amendements subséquents.

NL-339 (r. 88/04) c

Canada

UNIVERSITY OF ALBERTA

A SPECTROSCOPIC AND VISCOSIMETRIC INVESTIGATION OF THE STRUCTURE OF SILICATE MELTS

BY

© DAN SYKES

A THESIS SUBMITTED TO THE FACULTY OF GRADUATE STUDIES AND RESEARCH IN PARTIAL FULFILLMENT OF THE REQUIREMENTS FOR THE DEGREE OF DOCTOR OF PHILOSOPHY

DEPARTMENT OF GEOLOGY

EDMONTON, ALBERTA

SPRING, 1991

National Library of Canada
Bibliothèque nationale du Canada

Canadian Theses Service
Service des thèses canadiennes

Ottawa, Canada
K1A 0N4

The author has granted an irrevocable non-exclusive licence allowing the National Library of Canada to reproduce, loan, distribute or sell copies of his/her thesis by any means and in any form or format, making this thesis available to interested persons.

The author retains ownership of the copyright in his/her thesis. Neither the thesis nor substantial extracts from it may be printed or otherwise reproduced without his/her permission.

L'auteur a accordé une licence irrévocable et non exclusive permettant à la Bibliothèque nationale du Canada de reproduire, prêter, distribuer ou vendre des copies de sa thèse de quelque manière et sous quelque forme que ce soit pour mettre des exemplaires de cette thèse à la disposition des personnes intéressées.

L'auteur conserve la propriété du droit d'auteur qui protège sa thèse. Ni la thèse ni des extraits substantiels de celle-ci ne doivent être imprimés ou autrement reproduits sans son autorisation.

ISBN 0-315-66749-4

Canada

UNIVERSITY OF ALBERTA

RELEASE FORM

NAME OF AUTHOR: Dan Sykes

TITLE OF THESIS: A spectroscopic and viscosimetric investigation of the structure of silicate melts

DEGREE: Doctor of Philosophy

YEAR THIS DEGREE GRANTED: 1991

Permission is hereby granted to THE UNIVERSITY OF ALBERTA LIBRARY to reproduce single copies of this thesis and to lend or sell such copies for private, scholarly or scientific research purposes only.

The author reserves other publication rights, and neither the thesis nor extensive extracts from it may be printed or otherwise reproduced without the author's written permission.

Dan G. Sykes

228 McCarley Place

McKinney, Texas

USA 75070

Date: Nov. 20, 1990

THE UNIVERSITY OF ALBERTA

FACULTY OF GRADUATE STUDIES AND RESEARCH

The undersigned certify that they have read, and recommend to the Faculty of Graduate Studies and Research for acceptance, a thesis entitled A Spectroscopic and Viscosimetric Investigation of the Structure of Silicate Melts submitted by Dan Sykes in partial fulfilment of the requirements for the degree of Doctor of Philosophy.

.....

K. Muehlenbachs - Supervisor

.....

R. W. Luth

.....

H. Baadsgaard

.....

L. G. Hepler

.....

J. E. Bertie

.....

P. C. Hess - External Examiner

Date Nov 20 90

THIS THESIS IS DEDICATED TO THE MEMORY OF

CHRISTOPHER M. SCARFE

ABSTRACT

The Raman spectra of nine 0.1 MPa glass samples in the system nepheline-diopside are presented. Nepheline glass consists of a fully polymerized network structure with largely six-membered rings of Q^4 tetrahedra. The structure of diopside glass contains Q^0, Q^1, Q^2 and Q^3 units. Intermediate compositions with up to 18 mole% nepheline have Q^0, Q^1, Q^2, Q^3 and Q^4 structural units. Nepheline-rich compositions contain two discrete molecular structures with different polymerization modes (Q^2 and Q^4 units). This tendency to form molecular clusters is facilitated by the inability of Ca and Mg to compete with Na on nonframework sites in structural units having only bridging oxygens.

The viscosities of melts at 0.1 MPa in the system nepheline-diopside have been measured using rotational and beam-bending viscosimetric techniques. The large temperature dependence of the viscosity of diopside melt results from a change in the mechanism of viscous flow initially characterized by the motion of a distribution of flow units of various size, at high temperature, to one in which the size of the flow unit is effectively that of the macroscopic system at the glass transition. The weak temperature dependence of the viscosity of nepheline melt is a result of the initial paucity and large size of the flow units at high temperature. The low temperature viscosity minimum at intermediate compositions develops as a consequence of their different viscosity-temperature profiles.

^{27}Al, ^{29}Si MAS NMR, Raman, and IR spectroscopic techniques were employed to investigate the effect of pressure on the structure of orthoclase melt and to evaluate water solubility mechanisms in aluminosilicate melts. No evidence for six-coordinated aluminum was observed. Results for the anhydrous

glasses indicate that as pressure is increased, the distribution of T-O-T bond angles is reduced, leading to narrower peak widths at 480 cm^{-1} in the Raman spectra. This reduced distribution limits the ability of the network to compensate for the presence of three-membered rings and results in a distortion of the intertetrahedral linkages associated with these configurations. Aluminum in these energetically-unfavorable, three-membered rings may react preferentially with H_2O, forming Q^3-(OH) sites. This would be consistent with the observed changes in the ^{27}Al MAS NMR spectra. Changes in the high-frequency envelopes in the Raman and IR spectra are not consistent with the formation of Si Q^3-(OH) sites.

ACKNOWLEDGEMENTS

This thesis could not have been accomplished without the inspiration and friendship of Christopher M. Scarfe. Chris will be deeply missed.

The support and guidance of Karlis Muehlenbachs and Robert Luth are sincerely appreciated. They have offered much of themselves, with little reward, toward the completion of this degree. I hope that one day the favor can be returned.

I owe my Mother much for encouraging me to pursue a college education and my wife, Wanda, for being there during its completion.

Many thanks to my Experimental Petrology friends and coworkers: Dante Canil, Jim Dickinson Jr., Robert Sato, Brent Poe, Jonathan Stebbins and Paul McMillan.

Appreciation is also extended to my committee members John Bertie, Loren Hepler, Halfdan Baadsgaard and Paul Hess.

The experimental results presented here could not have been possible without the assistance of C.M. Scarfe and R.W. Luth (multianvil press and viscometer), J.E. Bertie (Raman spectrometer), J. Stebbins (MAS NMR spectrometer), P. McMillan (MAS NMR, microRaman, IR spectrometers), and the Geological Society of America (Graduate Research Grant #A8394).

TABLE OF CONTENTS

1. THESIS INTRODUCTION..... 1

1.4 References.....6

2. MELT STRUCTURE IN THE SYSTEM NEPHELINE-DIOPSIDE..... 9

2.1 Introduction.....9

2.2 Methods..... 9

2.3 Results.....10

2.4 Discussion.....14

2.5 Conclusion.....18

2.6 References.....24

3. VISCOSITY-TEMPERATURE RELATIONSHIPS AT .01MPa
IN THE SYSTEM NEPHELINE-DIOPSIDE.....28

3.1 Introduction.....28

3.2 Methods..... 29

3.3 Results.....31

3.4 Discussion.....32

3.5 Conclusion.....37

3.6 References.....44

4. A SPECTROSCOPIC INVESTIGATION OF THE STRUCTURE OF
ANHYDROUS AND HYDROUS $KAlSi_3O_8$ GLASSES QUENCHED
FROM HIGH PRESSURE.....46

4.1 Introduction.....46

4.2 Methods..... 47

4.3 Results.....51

4.4 Discussion..... 57

4.5 Conclusion..... 63

4.6 References.....74

5. THESIS CONCLUSION..... 79

5.1 References.....84

LIST OF TABLES

TABLE

2.1 Compositions of nepheline-diopside glasses..... 20

3.1 Log η - temperature results for nepheline-diopside glasses.....39

3.2 Fulcher equation constants for nepheline-diopside glasses..... 40

4.1 MAS NMR results for anhydrous and hydrous $KAlSi_3O_8$ glasses.....64

LIST OF FIGURES

FIGURE

2.1a Raman (parallel) spectra of nepheline-diopside glasses..... 21

2.1b Raman (perpendicular) spectra of nepheline-diopside glasses..... 22

2.2 Raman spectra of DN50 and DFO glasses.....23

3.1 Log η vs. reciprocal temperature for nepheline-diopside glasses..... 41

3.2 Log η vs. reciprocal temperature (full temperature range)..... 42

3.3 Log η vs. composition at selected isotherms..... 43

4.1 18M octahedral pressure assembly..... 65

4.2 Raman spectra of high pressure anhydrous $KAlSi_3O_8$ glasses..... 66

4.3 IR spectra of anhydrous and hydrous $KAlSi_3O_8$ glasses..... 67

4.4 ^{27}Al MAS NMR spectra of anhydrous $KAlSi_3O_8$ glasses..... 68

4.5 ^{27}Al MAS NMR spectra of 2 GPa hydrous $KAlSi_3O_8$ glasses..... 69

4.6 Raman spectra of anhydrous and hydrous $KAlSi_3O_8$ glasses..... 70

4.7 Difference spectra of 2 GPa hydrous $KAlSi_3O_8$ glasses..... 71

4.8 ^{29}Si MAS NMR spectra of 2 GPa hydrous $KAlSi_3O_8$ glasses.....72

4.9 ^{27}Al MAS NMR spectra of high pressure hydrous $KAlSi_3O_8$ glasses...73

1. THESIS INTRODUCTION

The atomic and molecular configuration of a substance, and the modification of this structure due to interactions with other materials, govern the thermal and physical properties of chemical systems. Silicates are an important class of chemicals where a knowledge of this relationship is fundamental for understanding the evolution of the Earth and other terrestrial planets. Igneous processes generally involve melting crystalline material; hence, characterization of the liquids involved provides a basis for understanding the mechanisms that shape our planet. Recent advances in analytical instrumentation and laboratory simulation techniques have permitted unprecedented correlations of the macroscopic properties of melts with the microscopic molecular and atomic interactions.

The purpose of this thesis is to provide a description of the structure of certain silicate melts using spectroscopic and viscosimetric techniques. Two chapters evaluate changes in the structure of the melt phase as a function of composition (chapter 2) and the effect these changes have on the viscosity of the melt phase (chapter 3). The fourth chapter investigates pressure-induced changes in the structure of the melt phase and the dependence of the mechanism of water solubility on the structure of the melt at high pressure.

1.1 Structure of $CaMgSi_2O_6$-$NaAlSiO_4$ Glasses

The melting of a mechanical mixture of chemical compounds results in an intermingling of possibly distinct structures between the endmember components. The degree of interaction determines such properties as thermal expansion, viscosity and density of the melt phase and liquidus phase relations.

Several techniques have been applied to monitor changes in structure with changing composition. For example, the Raman effect has been used extensively in the geological and glass sciences (see, for example, reviews by McMillan, 1984a and Mysen, 1988) to study structural variation in chemically related glasses as an aid in the development of use-specific materials, and for modeling crystal-melt equilibria.

In chapter 2, a Raman spectroscopic investigation of the structure of glasses in the system nepheline-diopside is reported. The structures of the endmember components and related compositions have been the subject of previous investigations of glasses in the systems Na_2O-Al_2O_3-SiO_2 and CaO-MgO-SiO_2 (Etchepare, 1972; Brawer and White, 1977; Seifert et al., 1982; Mysen et al., 1982; McMillan, 1984b). The reasonably coherent picture of the relationship between structural variation and composition emerging from the spectroscopic investigations of these simple systems can now provide a foundation for the interpretation of spectra of more complex multicomponent systems (e.g. nepheline-diopside). The present Raman spectroscopic study was undertaken to determine the mixing behavior of two compositions of widely contrasted polymerized modes. The system nepheline-diopside was chosen besause it is a synthetic analogue of alkaline basalts (Bowen, 1928), and unlike other diopside-aluminosilicate systems, olivine is a liquidus phase (Schairer et al., 1962). Melt structure and the role of aluminum are discussed and compared with the results of other spectroscopic and calorimetric investigations of chemically related systems.

1.2 Viscosity of Silicate Melts: Relationship to Structure

Viscous flow is the cumulative result of local rearrangements of the bond structure (Lacy, 1967). The viscosity of a melt, therefore, is dependent on the cooperative rearrangement of 'flow-units' and on the number of nonbridging oxygens. For example, a decrease in temperature results in an increase in melt viscosity because translational motion becomes sluggish and inhibits the number of possible cooperative rearrangements. The random network of nepheline melt has a high viscosity because all tetrahedra have four bridging oxygens, whereas diopside melt has a low viscosity because of a greater number of nonbridging oxygens bonded to a given tetrahedrally-coordinated silicon.

In chapter 3, the results of an investigation of the viscous properties of melts in the system nepheline-diopside are reported. The viscosity-temperature-composition relationships are discussed in the context of the structural interpretation in chapter 2. The results are compared to the viscous properties of related systems and qualitatively assessed using the configurational entropy theory of Adam and Gibbs (1965) and Richet (1984).

1.3 Solubility of Water and Coordination of Aluminum in Silicate Melts

Studies pertaining to the thermal and chemical structure of the earth require a knowledge of the effect of pressure on phase relations and physical properties of silicate materials. Pressure-induced changes in coordination of cations in crystalline silicates have been well documented (Akaogi et al., 1989; Katsura and Ito, 1989), and similar coordination changes have been proposed for melts (Waff, 1975; Kushiro, 1976, 1978; Boettcher et al., 1984). Aluminum has received a considerable degree of attention for several reasons. Firstly,

framework aluminosilicate melts are easily quenched to a homogeneous glass phase at high pressure , and secondly, pressure should induce a coordination change in the larger Al cation before the smaller Si cation. The chemical evolution of a melt, and its physical properties, may be significantly altered by the transformation of Al from four to six coordination. For example, the formation of immiscible regions may be facilitated by the exchange of network-modifying cations from Si tetrahedra to Al octahedra.

The dissolution of water produces significant changes in silicate mineralogy and in the properties of silicate melts at high pressure. Water decreases liquidus temperatures and increases the stability fields of depolymerized mineral structures relative to polymerized minerals (Yoder, 1958, 1965). Hydrous melts also have faster cation diffusion rates and lower viscosities than their anhydrous equivalents (Watson, 1981; Dingwell, 1987). In order to explain these features of hydrous melts, water solubility mechanisms in aluminosilicate systems generally invoke a disruption of the extended network and the production of nonbridging oxygens (Stolper, 1982; McMillan et al., 1983; Mysen and Virgo, 1986a,b). The formation of nonbridging oxygens in hydrous framework aluminosilicate melts may facilitate a change in the coordination of Al. For example, pressure-induced changes in Si coordination in high pressure SiO_2-Na_2O glasses are maximized at the sodium tetrasilicate composition (i.e. when the average number of nonbridging oxygens per tetrahedron equals one (X. Xue, pers. comm.)).

In chapter 4, a ^{27}Al, ^{29}Si MAS NMR, Raman, and IR spectroscopic investigation of anhydrous and hydrous $KAlSi_3O_8$ glasses quenched from high-pressure is reported. $KAlSi_3O_8$ was chosen because the structure of the glass at

.01 MPa is well characterized and the hydrous composition was quenchable at ≤7 GPa. Results are compared to previous investigations of anhydrous and hydrous albite glass. It was found that the proposed water solution mechanism was dependent on an accurate description of the structure of the high pressure anhydrous glass, which earlier investigations have ignored.

The investigations contained in this thesis assume that the structure of the glass is equivalent to that of the melt from which it is quenched. Several Raman and IR studies have shown that the .01 MPa glass and melt spectra are broadly similar and can be considered isostructural (Sweet and White, 1969; Sharma et al., 1978; Seifert et al., 1981). At present, it is not known if pressure-induced coordination changes in aluminosilicate glasses can be preserved during quenching. Ohtani et al. (1985) report the presence of high-coordinated Al in albite glasses quenched from high pressure and temperature. However, their results were not confirmed in a similar study of high pressure albite glasses by Stebbins and Sykes (1990). Williams and Jeanloz (1988) performed *in-situ* IR measurements on anorthite glass at room temperature produced from the amorphitization of crystalline anorthite, and found that coordination changes were not preserved at pressures below 8 GPa. The applicability of their room temperature study to the present investigation is unclear, because the process of amorphitization may differ from the formation of a glass by quenching from high temperature. Further *in-situ* studies at high pressure and high temperature may resolve these uncertainties.

1.4 REFERENCES

Adam, G. and Gibbs, J. (1965) On the temperature dependence of cooperative relaxation properties in glass-forming systems. J. Chem. Phys. **43**, 139-146.

Akaogi, M., Ito, E. and Navrotsky, A. (1989) Olivine-modified spinel-spinel transitions in the system Mg_2SiO_4-Fe_2SiO_4: calorimetric measurements, thermochemical calculation, and geophysical application. J. Geophys. Res. **94**, 15671-15685.

Boettcher, A., Guo, Q., Bohlen, S. and Hanson, B. (1984) Melting in feldspar-bearing systems to high pressures and the structures of aluminosilicate liquids. Geol. **12**, 202-204.

Bowen, N. (1928) The evolution of the igneous rocks. Princeton University Press, New Jersey.

Brawer, S. and White, W. (1977) Raman spectroscopic investigation of the structure of silicate glasses. II. Soda-alkaline earth-alumina ternary and quaternary glasses. J. Non-Cryst. Solids **23**, 261-278.

Etchepare, J. (1972) Study by Raman spectroscopy of crystalline and glassy diopside. In Amorphous Materials, ed. by Douglas, R. and Ellis, B., Wiley Interscience, 337-347.

Dingwell, D. (1987) Melt viscosities in the system $NaAlSi_3O_8$-H_2O-F_2O_{-1}. In Magmatic Processes: Physicochemical Principles, ed. by Mysen, B., Geochemical Society, 423-432.

Katsura, T. and Ito, E. (1989) The system Mg_2SiO_4-Fe_2SiO_4 at high pressures and temperatures: precise determination of stabilities of olivine, modified spinel, and spinel. J. Geophys. Res. **94**, 15663-15670.

Kushiro, I. (1978) Viscosity and structural changes of albite ($NaAlSi_3O_8$) melt at high pressures. Earth Planet. Sci. Lett. **41**, 87-90.

Kushiro, I. (1976) Changes in viscosity and structure of melt of $NaAlSi_2O_6$ composition at high pressures. J. Geophys. Res. **81**, 6347-6350.

Lacy, E. (1967) The newtonian flow of simple silicate melts at high temperature. Phys. Chem. Glass **8**, 238-246.

McMillan, P. (1984a) Structural studies of silicate glasses and melts-applications and limitations of Raman spectroscopy. Am. Min. **69**, 622-644.

McMillan, P. (1984b) A Raman spectroscopic study of glasses in the system CaO-MgO-SiO_2. Am. Min. **69**, 645-659.

McMillan, P., Jakobsson, S., Holloway, J. and Silver, L. (1983) A note on the Raman spectra of water-bearing albite glasses. Geochim. Cosmochim. Acta **47**, 1937-1943.

Mysen, B. (1988) Structure and properties of silicate melts. Elsevier Scientific Publishing Company, New York.

Mysen, B. and Virgo, D. (1986a) Volatiles in silicate melts at high pressure and temperature. 1. Interaction between OH groups and Si^{4+}, Al^{3+}, Ca^{2+}, Na^{+} and H^{+}. Chem. Geol. **57**, 303-331.

Mysen, B. and Virgo, D. (1986b) Volatiles in silicate melts at high pressure and temperature. 2. Water in melts along the join $NaAlO_2$-SiO_2 and a comparison of solubility mechanisms of water and fluorine. Chem. Geol. **57**, 333-358.

Mysen, B. Virgo, D. and Seifert, F. (1982) The structure of silicate melts: implications for chemical and physical properties of natural magma. Rev. Geophys. Space Phys. **20**, 353-383.

Ohtani, E., Taulelle, F. and Angell, C. (1985) Al^{3+} coordination changes in liquid aluminosilicates under pressure. Nature **314**, 78-81.

Richet, P. (1984) Viscosity and configurational entropy of silicate melts. Geochim. Cosmochim. Acta **48**, 471-483.

Schairer, J., Yagi, K. and Yoder, H., Jr. (1962) The system nepheline-diopside. CIWY **61**, 96-98.

Seifert, F., Mysen, B. and Virgo, D. (1981) Structural similarity of glasses and melts relevant to petrological processes. Geochim. Cosmochim. Acta **45**, 1879-1884.

Seifert, F., Mysen, B. and Virgo, D. (1982) Three-dimensional network structure of quenched melts (glass) in the systems SiO_2-$NaAlO_2$, SiO_2-$CaAl_2O_4$ and SiO_2-$MgAl_2O_4$. Am. Min. **67**, 696-717.

Sharma, S., Virgo, D. and Mysen, B. (1978) Structure of glasses and melts of Na_2O-$xSiO_2$ (x = 1,2,3) composition from Raman spectroscopy. CIWY **77**, 649-652.

Stolper, E. (1982) Water in silicate glasses: an infrared spectroscopic study. Cont. Min. Pet. **81**, 1-17.

Sweet, J. and White, W. (1969) Study of sodium silicate glasses and liquids by infrared spectroscopy. Phys. Chem. Glasses **10**, 246-251.

Waff, H. (1975) Pressure-induced coordination changes in magmatic liquids. Geophys. Res. Lett. **3**, 193-196.

Watson, E. (1981) Diffusion in magmas at depth in the earth: the effects of pressure and dissolved H_2O. Earth Planet. Sci. Lett. **52**, 291-301.

Williams, Q. and Jeanloz, R. (1988) Spectroscopic evidence for pressure-induced coordination changes in silicate glasses and melts. Science **239**, 902-905.

Yoder, H., Jr. (1965) Diopside-anorthite-water at five and ten kilobars and its bearing on explosive volcanism. CIWY **64**, 82-89.

Yoder, H., Jr. (1958) Effect of water on the melting of silicates. CIWY **57**, 189-191.

2. MELT STRUCTURE IN THE SYSTEM NEPHELINE-DIOPSIDE

2.1 INTRODUCTION

A knowledge of the structure of silicate melts is pertinent to our understanding of the physical and thermochemical properties governing the generation and evolution of magmatic liquids. This importance is evidenced by the number of spectroscopic tools that have been applied to probing atomic structure and molecular speciation (IR, Raman, MAS NMR, XAFS, XANES, and others).

The present Raman spectroscopic study investigates the structure of a number of glasses related by the mixing of Al-bearing (polymerized) and Al-free (depolymerized) melt compositions. The system $NaAlSiO_4$-$CaMgSi_2O_6$ was chosen because of its non-ideal mixing behavior (Schairer et al., 1962), and its usefulness as an analogue of alkaline magmas. The presence of olivine as a liquidus phase (Schairer et al., 1962) is unique, with respect to other diopside-aluminosilicate systems, and suggests that structural variation along this join may provide some insight on the thermochemical properties of the mixing process.

Results are discussed with regard to previous spectroscopic and calorimetric investigations of the end-members and related systems. The current results will be used as the basis for a later discussion concerning the viscous properties of these liquids.

2.2 METHODS

Glass samples were prepared from reagent grade oxides and carbonates. Silicic acid and Al_2O_3 were dried at 1400°C, MgO at 1200°C, and Na_2CO_3 and $CaCO_3$ at 500°C for six hours. Powders were then ground and mixed in a ball mill for one hour. Mixtures were placed in 500 cm^3 platinum crucibles and decarbonated at 900°C for twenty hours. Glasses were produced by heating the mixtures to 1650°C for four hours then pouring the melts onto a steel slab. All glasses, except DFO (see Table 2.1), were annealed at 600°C. All glasses were analyzed by Christine Payette at the University of Saskatchewan using a JEOL JXA 8600 Superprobe set up for wavelength dispersive analysis. Diopside, almandine and jadeite were used as standards and the data were reduced using a ZAF correction routine. Analyses of glass compositions are given in Table 2.1.

The Raman spectra of nine samples were collected using a Spex 1403 Raman spectrometer. Polished glass samples, approximately 3x3x3 mm, were excited with the 514.5 nm line of an Ar^+ laser having a source power of 300 mW at the sample. A 90° scattering geometry was used. Spectra were collected at 2 cm^{-1} steps with count times of 10 sec/step and using 4 cm^{-1} slits. A polarizer was mounted in front of an optical scrambler to measure the parallel and perpendicular components of the scattered radiation. The spectra were not corrected for background scattering.

2.3 RESULTS

The spectra for the end-members (Figure 2.1a,b) are similar to previously published results (Etchepare, 1972; McMillan et al., 1982; Seifert et al., 1982; Mysen et al., 1982; McMillan, 1984; Matson et al., 1986). Band

assignments are discussed in terms of vibrational modes in Q^n species, where Q represents a silicate or aluminate tetrahedron bonded to n number of bridging oxygens (Matson et al., 1983).

Nepheline

There are four dominant topological features in the spectrum of nepheline glass (Figure 2.1a,b). These features include two peaks in the low-frequency region at 490 cm^{-1} and 560 cm^{-1}, a broad mid-frequency envelope between 700 cm^{-1} and 800 cm^{-1}, and a high-frequency envelope between 900 cm^{-1} and 1100 cm^{-1}.

The intense polarized band at 490 cm^{-1} results from a delocalized vibrational mode involving the symmetric stretch of bridged oxygens in T-O-T linkages (Bates, 1972; Brawer, 1975; Sharma et al., 1981; McMillan et al., 1982). These T-O-T linkages form a fully polymerized network consisting of six-membered rings of tetrahedra (Taylor and Brown, 1979).

The intensity of the polarized 560 cm^{-1} peak increases with $NaAlO_2$-content on the SiO_2-$NaAlSiO_4$ join to a maximum at the composition of nepheline (Sharma et al., 1978; Virgo et al., 1980; Mysen et al., 1980; McMillan et al., 1982; Seifert et al., 1982). The origin of the 560 cm^{-1} band is controversial. McMillan et al. (1982) indicate the band arises from transverse oxygen motion in Al-O-Al linkages, while Matson and Sharma (1985) suggest the presence of a Al^{3+}-stabilized defect structure, the nature of which is not discussed. Henderson et al. (1985) assigned the 560 cm^{-1} band to vibrations in planar 3-membered

ring configurations similar to interpretations of the 606 cm^{-1} (Galeener, 1982) and 490 cm^{-1} (Revesz and Walrafen, 1983) bands of SiO_2.

A band group between 700-800 cm^{-1} is present in all fully polymerized glasses and is generally attributed to motion of the tetrahedral cation (Si,Al) within its oxygen cage (Laughlin and Joannopoulos, 1977; Sharma et al., 1984).

The high-frequency envelope between 900 cm^{-1} and 1100 cm^{-1} results from the antisymmetric stretching modes of Si-O bonds in Si-O-T linkages (Virgo et al., 1980; Mysen et al., 1980; McMillan et al., 1982; Matson and Sharma, 1985). The envelope is composed of at least two bands (960, 1080 cm^{-1}) with different depolarization ratios (Figure 2.1b).

Diopside

The low-frequency region of the spectrum of diopside glass (Figure 2.1a,b) has a broad envelope of weak intensity between 300 cm^{-1} and 500 cm^{-1}. Bands attributed to a rocking motion of the network modifying cations are believed to contribute to the intensity of this region (Etchepare, 1972). The strong polarized band at 637 cm^{-1} results from the symmetric stretch of Si-BO (bridged oxygen) bonds (Mysen et al., 1980; McMillan, 1984). The vibrational modes producing this band are thought to be highly localized, and therefore, preclude any interpretation of the intermediate-range order. However, the band is present in all glasses of metasilicate composition and may be used to indicate the presence of silicate tetrahedra with an average of two non-bridging oxygens (Q^2 species; Brawer and White, 1975; McMillan and Piriou, 1983).

The high-frequency envelope of diopside can be described in terms of combinations of four highly polarized bands at 1050 cm^{-1}, 970 cm^{-1}, 900 cm^{-1}, and 880 cm^{-1} (Figure 2.1b; McMillan, 1984). Previous studies on M_2O- and MO-SiO_2 glasses (Brawer and White, 1975; Verweij and Konijnendijk, 1976; Konijnendijk and Stevels, 1976; Kashio et al., 1980; Furukawa et al., 1981; Mysen et al., 1980, 1982; McMillan, 1984) indicate these bands result from symmetric silicon-oxygen stretching vibrations in silicate units with one (Q^3 species), two (Q^2 species), three (Q^1 species), and four (Q^0 species) nonbridging oxygens per tetrahedron, respectively.

Intermediate Compositions

The 490 cm^{-1} band of nepheline is resolved in spectra of compositions with as much as 66 mole% diopside (Figure 2.1a). The increased intensity in the low-frequency region of the spectra of DN82 and DN90 glasses relative to the spectra of diopside are consistent with the presence of the 490 cm^{-1} band in these spectra. There is no apparent shift in the frequency of the 490 cm^{-1} band with composition. The 560 cm^{-1} band seen in nepheline is present in all compositions except diopside. The ratio of the relative intensities of the 560 cm^{-1} and 490 cm^{-1} bands is constant between nepheline and DN18, then decreases at DN40 and remains constant between the spectra of DN40 and DN66.

The frequency of the 637 cm^{-1} band in diopside increases to 660 cm^{-1} in DN90 and DN82, and to 668 cm^{-1} in DN66 and DN50 (Figure 2.1a). This shift in the peak maximum to higher frequencies may be a result of the appearance of a band at 700 cm^{-1} resulting from stretching vibrations in Q^1 species (Lazarev,

1972). The increased intensity of this region in the cross-polarized spectra (Figure 1b), however, indicates the growth of a weakly polarized band, possibly related to the 700-800 cm^{-1} band group of nepheline. The growth of the mid-frequency envelope near 700 cm^{-1} obscures the presence of the 637 cm^{-1} band in nepheline-rich compositions.

In the high-frequency envelope, the intensities of the low- and high-frequency shoulders decrease relative to the peak maximum of the high-frequency envelope as nepheline content increases. In the spectrum of DN66, the low-frequency shoulder becomes unresolvable and the high-frequency shoulder is present only as an asymmetric tail on the high-frequency envelope (Figure 2.1a).

2.4 DISCUSSION

The melting of a diopside crystal disrupts the long-range order and periodicity of the crystalline lattice to produce a liquid with a variety of molecular structures. The distribution of these structures may be described by an equation relating the number of bridging oxygens of each molecular site (Virgo et al., 1980; Mysen et al., 1980, 1982, 1985; Murdoch et al., 1985)

$$Q^0 + Q^3 = Q^1 + Q^2 \quad (1).$$

The addition of nepheline introduces structural units containing only bridged oxygens (Q^4 species), which increases the bulk polymerization of the melt. A new equation is then necessary to describe the distribution of molecular structures

$$Q^0 + Q^4 = Q^1 + Q^3 \quad (2).$$

With continued addition of nepheline, the degree of polymerization is increased sufficiently for melt compositions to be represented by the equilibrium

$$2Q^3 = Q^2 + Q^4 \qquad (3).$$

Nepheline-diopside spectra may be interpreted in the context of the above equilibria. In DN90 and DN82, the increase in intensity of the 900 cm^{-1} band relative to the peak maximum of the high-frequency envelope, with increasing nepheline content, is consistent with an increase in Q^1 units (equation 2). Similarly, the growth of the high-frequency shoulder near 1050 cm^{-1} indicates an increase in Q^3 units (equation 2). Compared to the diopside spectrum, the intensity of the 880 cm^{-1} band in DN90 decreases relative to the peak maximum, consistent with a decrease in the number of Q^0 units.

The cross-polarized spectra of DN90 and DN82 (Figure 2.1b) indicate the presence of at least two depolarized bands near 960 cm^{-1} and 1080 cm^{-1} contributing to the intensity of the high-frequency envelope. These bands are associated with Si-BO vibrational modes in Q^4 tetrahedra and are consistent with the presence of Q^4 tetrahedra in DN90 and DN82 glasses.

Interpretation of features in the high-frequency envelope becomes difficult in compositions more nepheline-rich than DN82, because of the symmetric featureless character of the envelope (Figure 2.1a). However, the depolarized 1080 cm^{-1} and 960 cm^{-1} bands are evident in the cross-polarized spectra (Figure 2.1b). In DN66, the 1080 cm^{-1} and 960 cm^{-1} bands along with the 560 cm^{-1} and 480 cm^{-1} bands arise from stretching vibrations in Q^4 units, whereas, the 637 cm^{-1} band is associated with vibrational modes in Q^2 units. The presence of the 637 cm^{-1} band in DN66 indicates a band near 970 cm^{-1}, which

results from symmetric silicon-oxygen stretching vibrations in Q^2 silicate units, must also contribute to the intensity of the high-frequency envelope.

Previous studies (Mysen et al., 1982, 1985) have shown that compositions as polymerized as DN66 should have a distribution of Q^2, Q^3 and Q^4 silicate units (equation 3). In contrast, the present spectra indicate only two silicate units, Q^2 and Q^4. Stretching modes in Q^3 units produce intense bands near 1050 cm^{-1} and 570 cm^{-1}. The highly polarized character of these bands and their proximity to the 1080 cm^{-1} and 560 cm^{-1} bands of the Q^4 units may mask any contribution to the intensity of the spectra from Q^3 units. In order to determine the possible existence of unresolved bands resulting from stretching modes in Q^3 units, ten mole percent Mg_2SiO_4 (forsterite) was added to the DN50 glass (sample DFO). If Q^3 units are present, the addition of forsterite should depolymerize the glass and increase the proportion of Q^2 and Q^3 tetrahedra relative to Q^4 tetrahedra. This would result in an increase in the intensity of the spectrum at 1050 cm^{-1} and 570 cm^{-1} resulting from an increase in the proportion of Q^3 units. In contrast, a comparison of the spectra of DFO and DN50 (Figure 2) reveals only an increase in the intensity of the high-frequency envelope near 970 cm^{-1}, consistent with the presence of only Q^2 and Q^4 units.

The behavior of the low-frequency region (300-600 cm^{-1}) can be interpreted based on a model favoring smaller ring configurations with addition of diopside. Nepheline consists of a fully polymerized network structure of Q^4 tetrahedra. In crystalline nepheline, Al-avoidance (Loewenstein, 1954) is strictly obeyed (Stebbins et al., 1986; Stebbins, 1987) with each AlO_4-tetrahedron surrounded by four SiO_4-tetrahedra. However, the extra degrees of freedom in the glass phase allow for some Si-O-Si linkages with antisymmetric

stretching modes appearing at 1080 cm^{-1} in the glass spectra (Figure 2.1a,b; Matson and Sharma, 1985). The Si-O-Si linkages in nepheline glass may be concentrated preferentially in the three-membered ring configurations involving an AlO_4-tetrahedron. The assignment of the 560 cm^{-1} band to symmetric stretching modes in these smaller ring configurations (Henderson et al., 1985) is consistent with the studies of Galeener (1982), Revesz and Walrafen (1982) and Galeener and Geissberger (1983). Galeener (1982) calculated the optimum T-O-T bond angle in three-membered rings to be 130°, which is the same as the most stable Si-O-Al bond angle calculated by De Jong and Brown (1980).

These observations are consistent with the behavior of the 560 cm^{-1} band in the SiO_2-$NaAlSiO_4$ system. Substitution of NaAl for Si results in a decrease in the frequency and an increase in the intensity of the band (Seifert et al., 1982; McMillan et al., 1982), which would be a result of increased participation of the aluminate tetrahedra in the available three-membered rings. At nepheline, the intensity of the 560 cm^{-1} band reaches a maximum because every three-membered ring contains an AlO_4 tetrahedron.

Based on the evidence above, an increase in the ratio of the relative intensities of the 560/490 cm^{-1} bands between DN18 and DN40 (Figure 2.1a) would result from an increase in the number of smaller rings. The presence of a hidden band cannot account for the invariance in the position of the 560 and 490 cm^{-1} peaks nor can it account for the constant ratio of peak intensities between DN40-DN66 (including DFO).

The present interpretation of the vibrational spectra is consistent with a large portion (DN18-DN66) of the compositional join exhibiting a tendency to

unmix into discrete polymerized (Q^4) and depolymerized (Q^2) regions. This tendency towards incipient immiscibility has also been observed in the system SiO_2-$CaMgSi_2O_6$. McMillan (1984) suggests the clustering is a result of the reaction represented in equation (3) being driven to the right for small doubly-charged cations because of the higher charge concentration offered by the Q^2 site relative to the Q^3 site. Similarly, the formation of immiscible regions in nepheline-diopside and similar diopside-aluminosilicate systems may be related to mixing properties on the non-framework sites. Kleppa (1977) and Navrotsky et al. (1980) have shown that mixing of non-framework cations is most exothermic in the sequence Ca-Mg > Ca-Na > Ca-Mg-Na. This correlates well with heats of mixing in diopside-aluminosilicate systems. Diopside-anorthite and diopside-CaTs systems have negative heats of mixing (Navrotsky et al., 1980, 1983) and show no tendency to cluster into discrete polymerized and depolymerized regions (McMillan et al., 1982; Taniguchi and Murase, 1987). Positive heats of mixing (Navrotsky et al., 1980), glass-glass immiscibility (Henry et al., 1983), and molecular clustering (Dickinson and Scarfe, 1990) are characteristic of diopside-albite. The development of molecular clusters in diopside-nepheline and in diopside-albite is consistent with an inability of Ca and Mg to compete with Na to charge-balance fully polymerized aluminosilicate network structures (Roy and Navrotsky, 1984). It is suggested that the net heat effect observed in diopside-aluminosilicate systems depends on the mixing properties of the non-framework cations, with the magnitude of the heat effect depending on Al/(Al + Si) (Navrotsky et al., 1983).

2.5 CONCLUSION

Stretching modes in Q^0, Q^1, Q^2 and Q^3 sites contribute to the vibrational spectra of diopside glass. The addition of nepheline results in the appearance of bands associated with Q^4 sites, an increase in the intensities of the bands associated with the Q^1 and Q^3 sites, and a decrease in those arising from Q^0 and Q^2 sites. Nepheline-rich compositions (< 66 mole% diopside) contain only Q^2 and Q^4 tetrahedral sites. This molecular clustering is due to the inability of Ca and Mg to compete with Na as a charge-balancing cation. The present investigation suggests that the aluminate tetrahedra in nepheline glass are strongly partitioned into three-membered ring configurations, and that the proportion of these smaller rings increases with increasing diopside component.

Table 2.1 Compositions of nepheline-diopside glasses used in this study (DN90 = 90 mole% diopside + 10 mole% nepheline). Oxides are in weight percent. Samples were analyzed using a rastered 10 μm^2 diameter beam with an operating voltage of 15kV and a probe current of 10 nA. Compositions are an average of 5 analyses from each sample.

	Diop	DN90	DN82	DN66	DN50	DN40	DN18	Neph	DFO
SiO_2	55.39	53.92	52.72	50.59	48.41	47.07	44.77	42.56	47.49
Al_2O_3	-	4.41	7.55	14.00	19.85	24.30	30.37	35.91	19.27
MgO	18.39	16.62	14.32	11.25	7.69	6.01	2.61	-	10.91
CaO	25.71	22.54	20.21	16.02	11.00	8.93	3.83	-	10.95
Na_2O	-	2.72	4.68	8.10	12.21	14.61	18.33	21.67	11.44
total	99.49	100.21	99.48	99.96	99.16	100.92	99.91	100.19	100.06

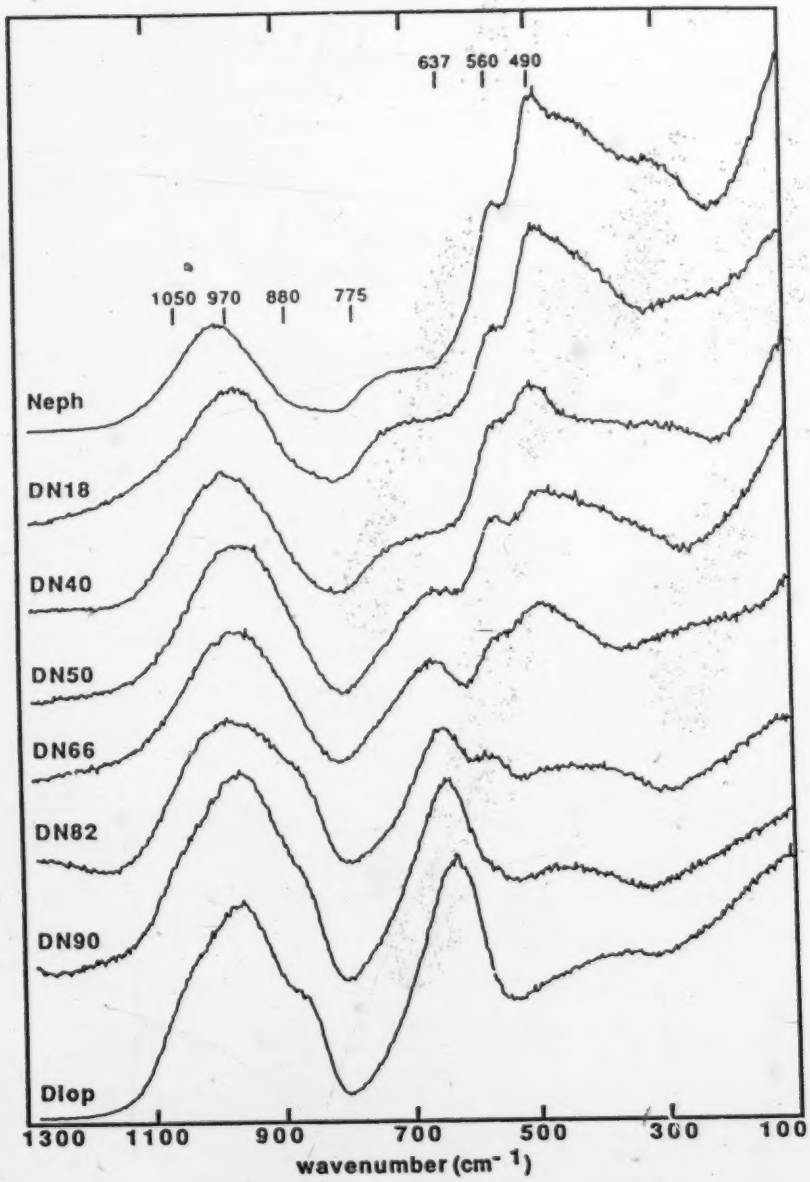

Figure 2.1 (a) Raman spectra of glasses in the system nepheline-diopside. Spectra are of the parallel component of the scattered radiation. Peak assignments are discussed in the text.

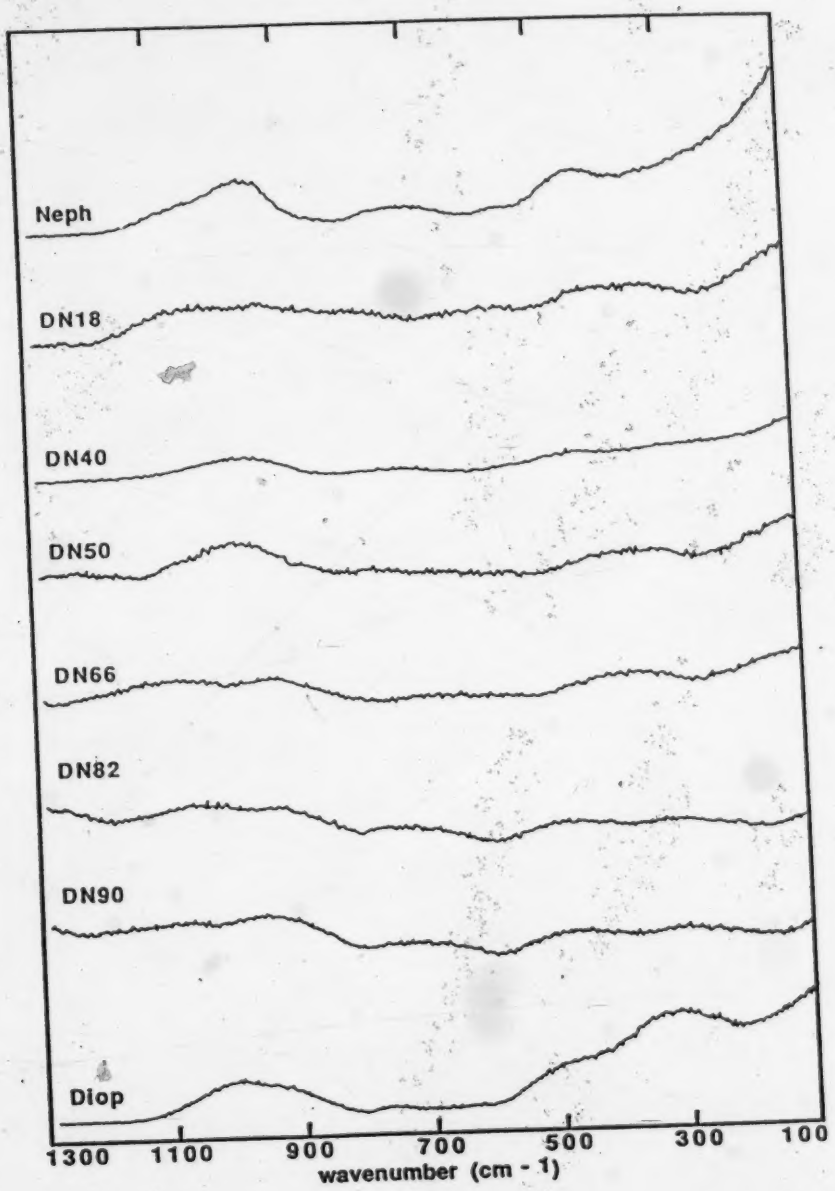

Figure 2.1 (b) Raman spectra of glasses in the system nepheline-diopside. Spectra are of the perpendicular component of the scattered radiation.

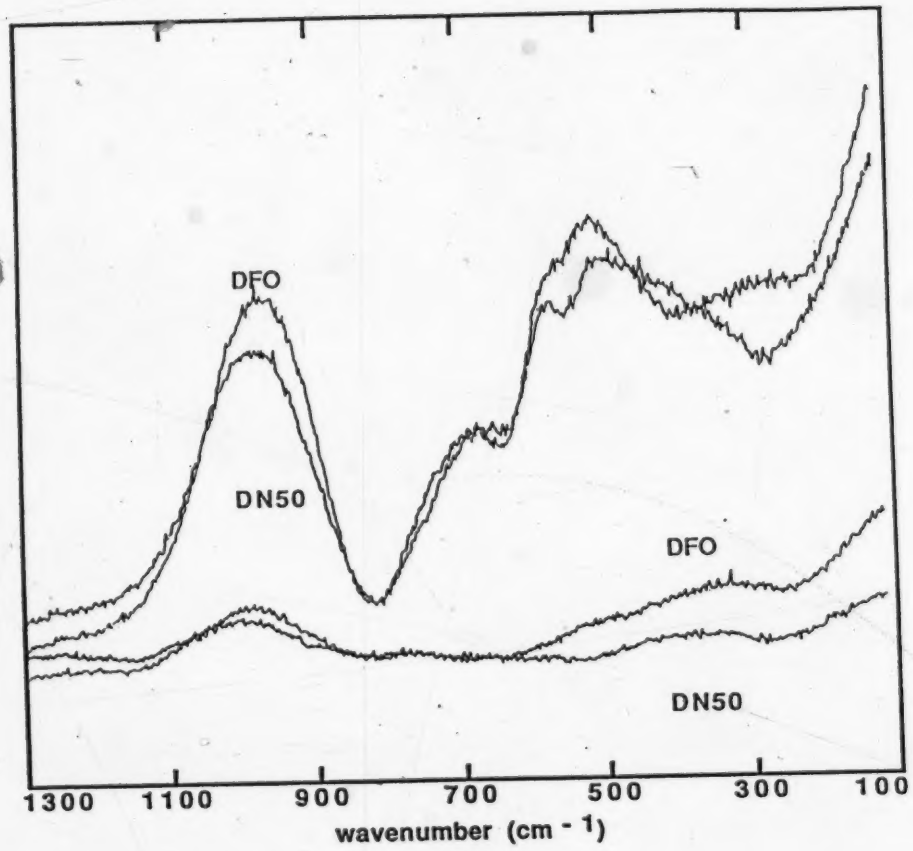

Figure 2.2 A comparison of the Raman spectra (parallel and perpendicular) of glasses DN50 and DFO (DFO = DN50 + 10 mole% forsterite).

2.6 REFERENCES

Bates, J. (1972) Dynamics of β-quartz structures of vitreous SiO_2 and BeF_2. J. Chem. Phys. **56**, 1910-1917.

Brawer, S. (1975) Theory of the vibrational spectra of some network and molecular glasses. Phys. Rev. B **11**, 3173-3194.

Brawer, S. and White, W. (1977) Raman spectroscopic investigation of the structure of silicate glasses. II. Soda-alkaline earth-alumina ternary and quaternary glasses. J. Non-Cryst. Solids **23**, 261-278.

Brawer, S. and White,W. (1975) Raman spectroscopic investigation of the structure of silicate glasses. I. The binary alkali silicates. J. Chem. Phys. **63**, 2421-2432.

De Jong, B. and Brown, G. (1980) The polymerisation of silicate and aluminate tetrahedra in glasses, melts and aqueous solutions- I. Electronic structure of $H_6Si_2O_7$, H_6AlSiO_7 and $H_6Al_2O_7$. Geochim. Cosmochim. Acta **44**, 491-511.

Dickinson, J., Jr. and Scarfe, C. (1990) Raman spectroscopic study of glasses on the join diopside-albite. Geochim. Cosmochim. Acta **54**, 1037-1044.

Etchepare, J. (1972) Study by Raman spectroscopy of crystalline and glassy diopside. in Amorphous Materials, ed. by Douglas, R. and Ellis, B. Wiley Interscience, 337-347.

Furukawa, T., Fox, K. and White, W. (1981) Raman spectroscopic investigation of the structure of silicate glasses. III. Raman intensities and structural units in sodium silicate glasses. J. Chem. Phys. **75**, 3226-3237.

Galeener, F. (1982) Planar rings in glasses. Solid State Comm. **44**, 7, 1037-1040.

Galeener, F. and Geissberger, A. (1983) Vibrational dynamics in ^{30}Si-substituted vitreous SiO_2. Phys. Rev. B **27**, 6199-6204.

Henderson, G., Bancroft, G., Fleet, M. and Rogers, D. (1985) Raman spectra of gallium and germanium substituted silicate glasses: variations in intermediate-range order. Am. Min. **70**, 946-960.

Henry, D., MacKinnon, I., Chan, I. and Navrotsky, A. (1983) Subliquidus glass-glass immiscibility along the albite-diopside join. Geochim. Cosmochim. Acta **47**, 277-282.

Kashio, S., Iguchi, Y., Goto, T., Nishina, Y. and Fuwa, T. (1980) Raman spectroscopic study on the structure of silicate slag. Trans. Iron Steel Inst. Japan **20**, 251-253.

Kleppa, O. (1977) Thermodynamic properties of molten salt solutions. In Thermodynamics in Geology, ed. by Fraser, D., D. Reidel Publ. Co., 279-300.

Konijnendijk, W. and Stevels, J. (1976) Raman scattering measurements of silicate glasses and compounds. J. Non-Cryst. Solids **21**, 447-453.

Laughlin, R. B. and Joannopoulos, J. D. (1977) Phonons in amorphous silica. Phys. Rev. B **16**, 2942-2952.

Lazarev, A. (1972) Vibrational spectra and structure of silicates. Consultants Bureau, New York.

Loewenstein, W. (1954) The distribution of aluminum in the tetrahedra of silicates and aluminates. Am. Min. **39**, 92-96.

Matson, D. and Sharma, S. (1985) Structures of sodium alumino- and gallosilicate glasses and their germanium analogs. Geochim. Cosmochim. Acta **49**, 1913-1924.

Matson, D., Sharma, S. and Philpotts, J. (1986) Raman spectra of some tectosilicates and of glasses along the orthoclase-anorthite and nepheline-anorthite joins. Am. Min. **71**, 694-704.

Matson, D, Sharma, S. and Philpotts, J. (1983) The structure of high-silica alkali-silicate glasses: a Raman spectroscopic investigation. J. Non-Cryst. Solids **58**, 323-352.

McMillan, P. (1984) A Raman spectroscopic study of glasses in the system CaO-MgO-SiO_2. Am. Min. **69**, 645-659.

McMillan, P. and Piriou, B. (1983) Raman spectroscopic studies of silicate and related glass structure- a review. Bull. Mineral. **106**, 57-75.

McMillan, P., Piriou, B. and Navrotsky, A. (1982) A Raman spectrscopic study of glasses along the joins silica-calcium aluminate, silica-sodium aluminate, and silica-potassium aluminate. Geochim, Cosmochim. Acta **46**, 2021-2037.

Murdoch, J., Stebbins, J. and Carmichael, I. (1985) High-resolution ^{29}Si NMR study of silicate and aluminosilicate glasses: the effect of network modifying cations. Am. Min. **70**, 332-343.

Mysen, B., Virgo, D. and Seifert, F. (1985) Relationships between properties and structure of aluminosilicate melts. Am. Min. **70**, 88-105.

Mysen, B., Virgo, D. and Seifert, F. (1982) The structure of silicate melts: implications for chemical and physical properties of natural magma. Rev. Geophys. Space Phys. **20**, 353-383.

Mysen, B., Virgo, D. and Scarfe, C. M. (1980) Relations between the anionic structure and viscosity of silicate melts- a Raman spectroscopic study. Am. Min. **65**, 690-710.

Navrotsky, A., Zimmermann, H. and Hervig, R. (1983) Thermochemical study of glasses in the system $CaMgSi_2O_6$-$CaAl_2SiO_6$. Geochim. Cosmochim. Acta **47**, 1535-1538.

Navrotsky, A., Hon, R., Weill, D. and Henry, D. (1980) Thermochemistry of glasses and liquids in the systems $CaMgSi_2O_6$-$CaAlSi_2O_8$-$NaAlSi_3O_8$, SiO_2-$CaAl_2S_2O_8$-$NaAlSi_3O_8$ and SiO_2-Al_2O_3-CaO-Na_2O. Geochim. Cosmochim. Acta **44**, 1409-1423.

Revesz, A. and Walrafen, G. (1983) Structural interpretations for some Raman lines from vitreous silica. J. Non-Cryst. Solids **54**, 323-333.

Roy, B., and Navrotsky, A. (1984) Thermochemistry of charge-coupled substitutions in silicate glasses: the systems $M_{1/n}$ AlO_2-SiO_2 (M= Li, Na, K, Rb, Cs, Mg, Ca, Sr, Ba, Pb). J. Am. Ceram. Soc. **67**, 606-610.

Schairer, J., Yagi, K. and Yoder, H. Jr. (1962) The system nepheline-diopside. CIWY **61**, 96-98.

Seifert, F., Mysen, B. and Virgo, D. (1982) Three-dimensional network structure of quenched melts (glass) in the systems SiO_2-$NaAlO_2$, SiO_2-$CaAl_2O_4$, and SiO_2-MAl_2O_4. Am. Min. **67**, 696-717.

Sharma, S., Matson, D., Philpotts, J. and Roush, T. (1984) Raman study of the structure of glasses along the join SiO_2-GeO_2. J. Non-Cryst. Solids **68**, 99-114.

Sharma, S., Mammone, J. and Nicol, M. (1981) Raman investigation of ring configurations in vitreous silica. Nature **292**, 140-141.

Sharma, S., Virgo, D. and Mysen, B. (1978) Structure of melts along the join SiO_2-$NaAlSiO_4$ by Raman spectroscopy. Carn. Inst. Wash. Ybk. **77**, 652-658.

Stebbins, J. (1987) Aluminum avoidance avoided. Nature **330**, 13-14.

Stebbins, J., Murdoch, J., Carmichael, I. and Pines, A. (1986) Defects and short-range order in nepheline group minerals: a silicon-29 nuclear magnetic resonance study. Phys. Chem. Min. **13**, 371-381.

Taniguchi, H. and Murase, T. (1987) Some physical properties and melt structures in the system diopside-anorthite. J. Volc. Geotherm. Res. **34**, 51-64.

Taylor, M. and Brown, G. Jr. (1979) Structure of mineral glasses-II. The SiO_2-$NaAlSiO_4$ join. Geochim. Cosmochim. Acta **43**, 1467-1473

Verweij, H. and Konijnendijk, W. (1976) Structural units in K_2O-PbO-SiO_2 glasses by Raman spectroscopy. J. Am. Ceram. Soc. **59**, 517-521.

Virgo, D., Mysen, B. and Kushiro, I. (1980) Anionic constitution of 1-atmosphere silicate melts: implications for the structure of igneous melts. Science **208**, 1371-1373.

3. VISCOSITY-TEMPERATURE RELATIONSHIPS AT 0.1 MPa IN THE SYSTEM NEPHELINE-DIOPSIDE

3.1 INTRODUCTION

The viscous properties of magmas are important parameters governing the generation and evolution of igneous rocks. For example, magmatic processes such as the formation and separation of melt from the source, convection, crystal fractionation, diffusion, and magma mixing are dependent on the viscosity of the molten phase. It is evident that the successful development of petrogenetic models relies on an understanding of the mechanism of viscous flow in igneous systems.

Viscous flow can be interpreted within the context of the configurational entropy model of relaxation processes (Adam and Gibbs, 1965; Richet, 1984), which states that the viscosity is inversely proportional to the configurational entropy of the melt. Investigations of the viscous behavior of feldspar and diopside composition melts using the configurational entropy model have successfully reproduced the viscosity-temperature relationships on a quantitative basis (Richet, 1984; Hummel and Arndt, 1985; Tauber and Arndt, 1986, 1987). Unfortunately, quantitative descriptions require thermodynamic data not readily available for most silicate compositions. In lieu of the necessary thermodynamic information, a knowledge of the structure of the melt combined with the viscosity-temperature data can provide important insights into the mechanisms of viscous flow, and to first order, the temperature and compositional dependence of the configurational entropy.

In the present paper, the viscous properties of melts in the system

$NaAlSiO_4$-$CaMgSi_2O_6$ (Ne-Di) are reported. The viscosity-temperature-composition relationships are discussed with reference to the structure of the glasses reported in Chapter 2 (Sykes and Scarfe, 1990). The results are compared to the viscous properties of related systems and qualitatively assessed using the configurational entropy model of Adam and Gibbs (1965) and Richet (1984).

3.2 METHODS

Glass compositions were prepared from reagent grade oxides and carbonates. Silicic acid and Al_2O_3 were dried at 1400°C, MgO at 1200°C, and Na_2CO_3 and $CaCO_3$ at 500°C for six hours. Powders were then ground and mixed in a ball mill for one hour. Glasses were produced by loading the mixtures in 500 cm^3 platinum crucibles and heating to 1650°C for four hours then pouring the melts onto a steel slab. The samples used for viscometry are from the same starting material as the samples used in Chapter 2. Compositions are given in Table 2.1.

High-temperature melt viscosities were monitored using Brookfield LVTD and HBTD rotational viscometers. Measurements were performed by rotating a Pt20Rh spindle (0.5 cm diameter, conical ends), immersed to a fixed depth, inside a Pt20Rh crucible (3.5 cm diameter) used to contain the melt. The torque, or viscous drag, exerted on the spindle is measured by the deflection of a calibrated spring attached to the pivot shaft. The angular displacement is converted to a millivolt signal and displayed by digital readout on the viscometer head. Melt viscosities were determined from a set of calibration curves derived

from NBS standard glasses 710 and 711. The accuracy and precision of the measurements were obtained from alternating determinations of the viscosities of the standard and sample glasses. Viscosities are accurate to ±5% with a precision of ±3%.

Measurements were performed over the temperature range 1250-1500°C. Viscosities were recorded at successively lower temperatures at intervals of 25°C or 50°C, after one hour equilibration times. Measurements were repeated over the same intervals up-temperature. Thermal equilibration of the sample was gauged by the invariance of the viscometer readout over a five minute interval. Temperatures were monitored using a Pt-Pt13Rh thermocouple located adjacent to the sample crucible and in the hot zone of a $MoSi_2$ furnace. Temperatures in the hot zone were uniform throughout the length of the crucible and have uncertainties of ±5°C. The viscosity-temperature relationship for nepheline melt could not be determined due to its high melting temperature. The nepheline melt viscosities reported by Riebling (1966) are used instead.

Low-temperature (supercooled) melt viscosities were measured at Corning Glass Works, courtesy of Dr. J. Dickinson Jr., with a custom-built beam-bending viscometer designed after Hagy (1967). Measurements were performed by recording the deflection of rectangular glass beams (5.3x0.3x0.3 cm) as a function of time. Cooling rates of -300°C/hour and a load weight of 243.7 g were employed. Viscosity and temperature were recorded at regular intervals and stored electronically. The instrument was calibrated using NBS standard glasses 710 and 711. Viscosities are accurate to ±6% with a precision of ±3%. Temperatures were monitored using a Pt-Pt13Rh thermocouple and have uncertainties of ±1°C.

3.3 RESULTS

Viscosity-temperature data are given in Table 3.1. The fundamental unit of viscosity measurement is the poise, which is equivalent to 0.1 Pa-s. Accordingly, the results are presented in the form of the log of the coefficient of viscosity (log η); the viscosity measured in units of poise. Viscosities for each composition were independent of shear rate (0.1 s^{-1} to 20 s^{-1}), indicating Newtonian behavior. High-temperature melt viscosities decrease with increasing temperature, and at constant temperature, decrease with increasing diopside component (Figure 3.1). Log η versus reciprocal temperature relationships for melt compositions with more than 50 mole% diopside are nonlinear. For compositions DN10 and DN30, the temperature dependence of the viscosity is Arrhenius (Figure 3.1). The present results for the viscosity of diopside melt are lower than the values reported by Scarfe et al. (1983), but agree within the combined uncertainties.

The low-temperature (supercooled) melt viscosities are recorded in Table 3.1 and presented in Figure 3.2. In contrast to the high-temperature results, there is an isothermal viscosity minimum at low temperature (Figure 3.3). The combined data sets show the log η-reciprocal temperature relationships for all compositions are nonlinear (Figure 3.2) and best fit by the Tamman-Vogel-Fulcher (TVF) equation (Fulcher, 1925)

$$\log \eta = A + B/(T-T_o) \qquad (1)$$

where η is the viscosity in poise and A, B, and T_o are adjustable parameters (Table 3.2).

3.4 DISCUSSION

Viscosity and Composition

One method of evaluating the viscous behavior of melts is to relate the viscosity to the degree of polymerization. NBO/T (nonbridging oxygens to tetrahedrally coordinated cations) is a measure of the degree of polymerization of a silicate melt and can be calculated from its bulk chemistry (Mysen et al., 1982). Nepheline has an NBO/T of 0 and is considered fully polymerized, whereas diopside has an NBO/T of 2 and is considered depolymerized. The lower melt viscosities with increasing diopside component (Figure 3.1) reflect this decrease in bulk polymerization. This dependence is also expressed in the systems $NaAlSi_3O_8$-$CaMgSi_2O_6$ (Ab-Di; Scarfe and Cronin, 1986) and $CaAl_2Si_2O_8$-$CaMgSi_2O_6$ (An-Di; Scarfe et al., 1983), where melt viscosities increase with increasing feldspar component (NBO/T=0). Similarly, the viscosities of melts in simple binary MO, M_2O-SiO_2 systems increase with SiO_2 because of an increase in the number of Si-O-Si intertetrahedral linkages, and consequently, a more polymerized melt structure (Shartsis et al., 1952; Bockris and Lowe, 1954; Bockris et al., 1955).

The mechanism of viscous flow in silicate melts is the cumulative result of local rearrangements of the bond structure (Lacy, 1967). Viscous flow proceeds by the translational and rotational motion of flow units formed by the disruption of the silicate melt structure (Seddon, 1939; Lacy, 1967). The concept of a flow unit is not rigorously defined, but the size of the flow unit can

be related to the degree of polymerization of the melt phase. Flow is initiated when the thermal energy of the system becomes sufficient to overcome the potential energy barriers of local bond configurations (Hummel and Arndt, 1985). Accordingly, the weak Si-O-M linkages (silicon-nonbridging, Si-NBO, bonds) are preferentially broken and act as the focal points of the flow process. Consequently, the size of the flow units decrease with increasing NBO/T which corresponds to the decrease in melt viscosity with increasing NBO/T (Mysen et al., 1980).

Melts of orthosilicate composition have the most deploymerized compositions (NBO/T=4) in the system M_2SiO_4-SiO_2. The melt structure can be described as consisting predominately of isolated silicate tetrahedra bounded by four nonbridging oxygens (Q^0 tetrahedra where Q^n is a tetrahedron with n bridging oxygens). As such, the size of the flow units may be of the scale of individual tetrahedron. Melts of diopside composition contain more polymerized tetrahedra (Q^0, Q^1, Q^2 and Q^3 tetrahedra; Mysen et al., 1980; McMillan, 1984). Two possibilities exist for the increase in viscosity from orthosilicate compositions to the more polymerized diopside (metasilicate) composition. First, the size of the flow units remain that of isolated tetrahedra and that flow becomes more difficult because stronger silicon-bridging oxygen (Si-BO) bonds must be overcome. And second, flow remains concentrated along Si-NBO bonds so that the average size of the flow unit must increase. The latter observation is consistent with the conclusion of Mysen et al. (1980) that the increase in activation energy with decreasing M/Si in MO, M_2O-SiO_2 systems results from an increase in the average size of the flow unit. Viscous flow in diopside melt may be controlled by a distribution of flow units of various size ranging from isolated tetrahedra (Q^0)

to units consisting of several tetrahedra (combinations of Q^1, Q^2 and Q^3 tetrahedra).

Melts on the join SiO_2-$NaAlSiO_4$ have a fully polymerized network structure consisting of six-membered rings of Q^4 tetrahedra (Taylor and Brown, 1979b). As there are no nonbridging oxygens, viscous flow must occur by a significantly different mechanism than in more depolymerized compositions. The decrease in melt viscosities with increasing Al/Si (Riebling, 1966) may be attributed to the increase in the number of Al-BO bonds, and therefore, a decrease in the average strength of the bridging bonds that must be broken to initiate viscous flow (Mysen et al., 1980; Dingwell, 1986). Anorthite is a fully polymerized network structure consisting of four-membered rings of Q^4 tetrahedra (Taylor and Brown, 1979a) and has the same Al/Si ratio as nepheline. The larger high temperature viscosity of nepheline may result from its larger six-membered ring configuration and suggests that the mechanism of viscous flow in fully polymerized network structures may depend on ring size.

It is suggested that the addition of nepheline to diopside melt results in a progressive increase in the degree of polymerization of the flow units and an increase in the viscosity of the melt. The mechanism of viscous flow changes from one initially characterized by a distribution of flow units of limited size and bounded by nonbridging oxygens to one in which the flow units are of the size of the ring complexes of the network structure of nepheline.

The systems $Na_2Si_2O_5$-$Na_4Al_2O_5$ (NS-NA), $K_2Si_3O_7$-$Na_2Si_3O_7$ (KS_3-NS_3) maintain constant bulk polymerization values of 1.0 and 0.67, respectively. Their viscosity minima at intermediate compositions (Richet, 1984; Dingwell, 1986) result from cation site-disorder similar to the mixed

alkali effect' in molten salt solutions (Isard, 1969; Richet, 1984). A 'mixed alkali effect' may contribute to the low temperature viscosity minimum in Ne-Di (Figure 3.3), however, the minimum primarily results from the greater temperature dependence of the viscosity of diopside melt relative to nepheline-rich melt. Similarly, Hummel and Arndt (1985) have interpreted the low temperature viscosity minimum in $NaAlSi_3O_8$-$CaAl_2Si_2O_8$ (Ab-An) in terms of the greater temperature dependence of the viscosity of anorthite to that of albite. Initially at high temperature, the viscosity of albite melt is several orders of magnitude larger than that of anorthite (Cukierman and Uhlmann, 1973; Cranmer and Uhlmann, 1981a,b).

Viscosity and Temperature

The disparate low and high temperature viscosity-composition relationships in Ne-Di (and Ab-An) suggest that composition- and temperature-induced polymerization influence viscous flow. Indeed, Uhlmann (1972) recognized that molecular shape (and distribution of tetrahedral configurations), type of bonding, and flexibility of the intertetrahedral linkages may all be important factors controlling viscous flow, and that their relative contributions may be largely temperature dependent. Scarfe et al. (1983) and Scarfe and Cronin (1986) have suggested that the viscosity-temperature-composition profiles in An-Di and Ab-Di may result from significant temperature-induced structural changes in diopside melt. Their conclusion is based on the pronounced temperature dependence of the activation energy for viscous flow of diopside melt relative to anorthite- and albite-rich compositions.

The two most common expressions used to represent viscosity-temperature data are the TVF (Fulcher, 1925) and configurational entropy equations (Richet, 1984). The TVF equation (1) is a strictly empirical formulation used to describe the temperature dependence of the viscosity. The limitations of the TVF equation have been reviewed by Hummel and Arndt (1985) and will not be discussed further. The configurational entropy equation

$$\log \eta = A_e + B_e/TS_{conf + mix} \qquad (2)$$

contains two adjustable parameters, A_e and B_e. For most silicate melts the necessary thermodynamic data (heat capacity) is not available to evaluate the configurational entropy ($S_{conf + mix}$). In such cases it must be assumed adjustable. However, the equation has consistently provided better fits to viscosity-temperature data than the TVF equation and is as yet the only model that is based on thermodynamic data (Richet, 1984; Hummel and Arndt, 1985; Tauber and Arndt, 1986, 1987).

According to the configurational entropy theory of Adam and Gibbs (1965), material transport in liquids takes place by cooperative rearrangements of the melt structure and depends on the number of configurations attainable by the system (Hummel and Arndt, 1985). The large increase in relaxation times near the glass transition is associated with the decrease to very small values in the number of configurations available to the system (Adam and Gibbs, 1965). $S_{conf + mix}$ is considered a measure of the temperature dependence of the number, and consequently, the size of the configurations. At the glass transition, only one configuration is available to the system, such that, relaxation times become infinite and S_{conf} reduces to zero (Richet, 1984).

The configurational entropy model provides a thermodynamic basis for the temperature dependence of the size of the flow unit (configuration). As the glass transition is approached, the potential energy barriers to viscous flow are not as easily overcome which results in a decrease in the number and an increase in the effective size of the flow units. For example, the large temperature dependence of the viscosity of diopside melt results from a change in the mechanism of viscous flow initially characterized by the motion of a distribution of flow units of various size, at high temperature, to one in which the size of the flow unit is effectively that of the macroscopic system at the glass transition. In contrast, the weaker temperature dependence of the viscosity of nepheline melt is a result of the initial paucity and large size of the flow units at high temperature.

The lack of a low temperature viscosity minimum in An-Di suggests that the temperature-dependence of the viscosity is equally dependent on the size of the Q^4 ring configurations in fully polymerized melts as it is on the degree of melt polymerization. This is evident in the system Ne-An where a low temperature viscosity minimum is predicted given the presence and absence of a viscosity minimum in Ne-Di and An-Di, respectively. The low temperature viscosity-composition profiles in Ne-Di and An-Di melts can be reconciled in the context of the above temperature dependence of the viscosities of these melts.

3.5 CONCLUSION

At high temperature, melt viscosities decrease with increasing diopside component. This decrease in melt viscosity can be attributed to a reduction in the size of the flow units due to an increase in the number of nonbridging oxygens per

tetrahedron. The low temperature viscosity minimum is a result of the larger temperature dependence of the viscosity of diopside relative to the viscosity of nepheline melt. The large temperature dependence of the viscosity of diopside melt results from a change in the mechanism of viscous flow initially characterized by the motion of a distribution of flow units of various size, at high temperature, to one in which the size of the flow unit is that of the macroscopic system at the glass transition. The weak temperature dependence of the viscosity of nepheline melt is a result of the large size of the flow units even at high temperature.

The temperature dependence of the viscosities of fully polymerized network structures depends on the size of the tetrahedral rings. The temperature dependence is greater for the four-membered ring configuration of anorthite than for the six-membered ring configuration of albite and nepheline. It is unclear, however, the effect the type of charge-balancing cation may have on the form of the temperature dependence (Mysen et al., 1980).

Table 3.1. Log viscosity-temperature results for nepheline-diopside melts.

T°C	Diop	DN90	DN70	DN50	DN30	DN10
1500	0.65	0.93	1.40	1.43	1.92	2.38
1475	0.71	-	-	-	-	2.48
1450	0.77	1.02	1.48	1.49	2.13	2.62
1425	0.87	-	-	-	-	2.76
1400	0.98	1.16	1.59	1.59	2.36	2.88
1375	-	1.21	-	1.67	-	-
1350	-	1.29	1.76	1.73	2.63	-
1325	-	1.40	1.87	1.81	2.75	-
1300	-	-	2.01	1.94	2.90	-
1275	-	-	2.14	2.07	3.03	-
1250	-	-	2.25	2.21	3.17	-
715	-	11.46	10.24	10.24	10.68	12.55
700	-	12.00	10.87	10.83	11.24	12.97
675	-	12.99	11.92	11.79	12.13	13.65

Table 3.2. Fulcher equation constants for the combined high- and low-temperature data.

	A	B	T_o
Diop	-1.07	1053	1157
DN90	-6.46	9079	482
DN70	-4.59	7103	515
DN50	-5.09	7910	476
DN30	-4.82	8942	422
DN10	-6.39	12596	324
Neph[a]	-6.32	16217	

[a] Arrhenius constants from Riebling (1966)

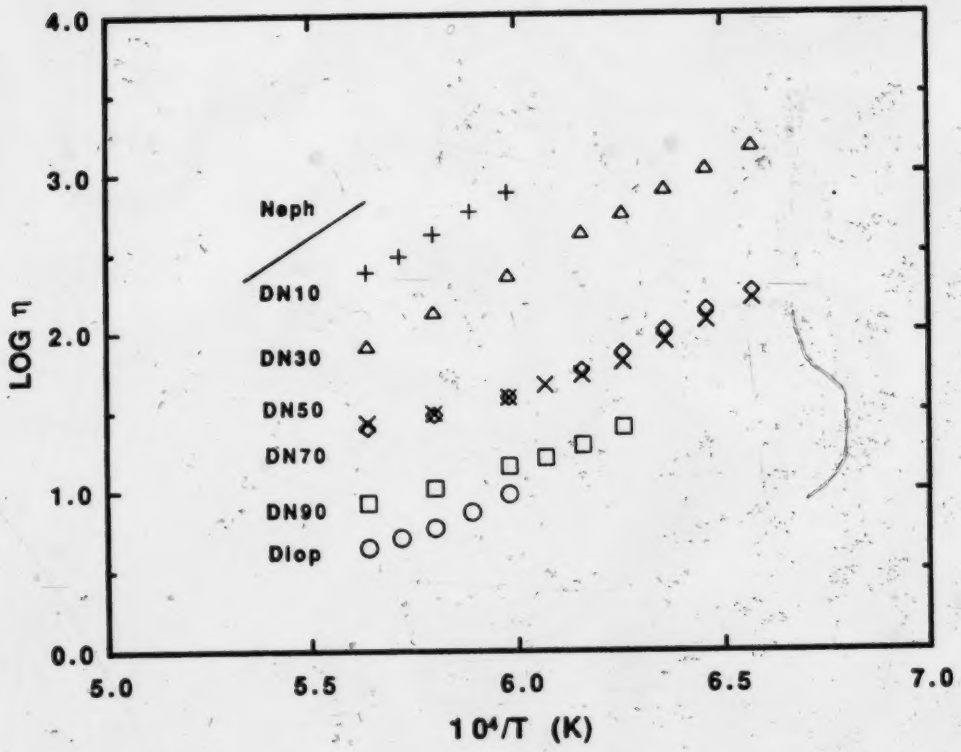

Figure 3.1 Log of the coefficient of viscosity (log η) vs. reciprocal temperature for high temperature melt viscosities. Data for nepheline is from Riebling (1966).

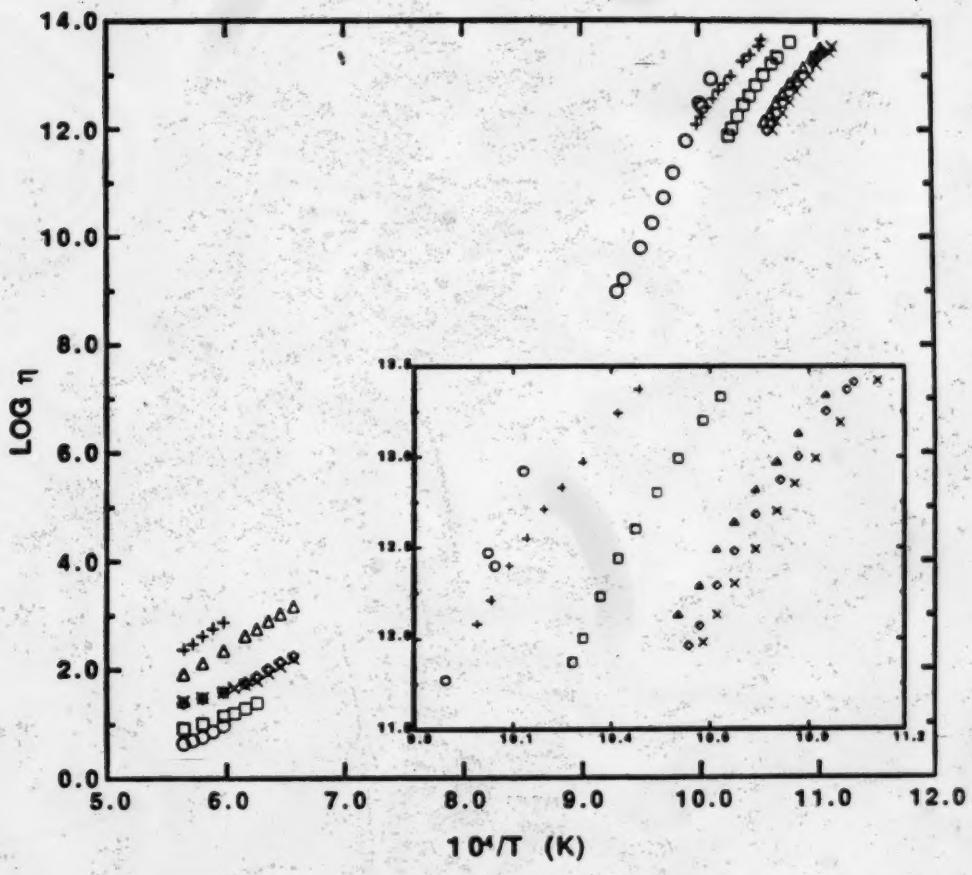

Figure 3.2 Log of the coefficient of viscosity (log η) vs. reciprocal temperature for combined data set. Diopside low temperature melt viscosities are from Tauber and Arndt (1986).

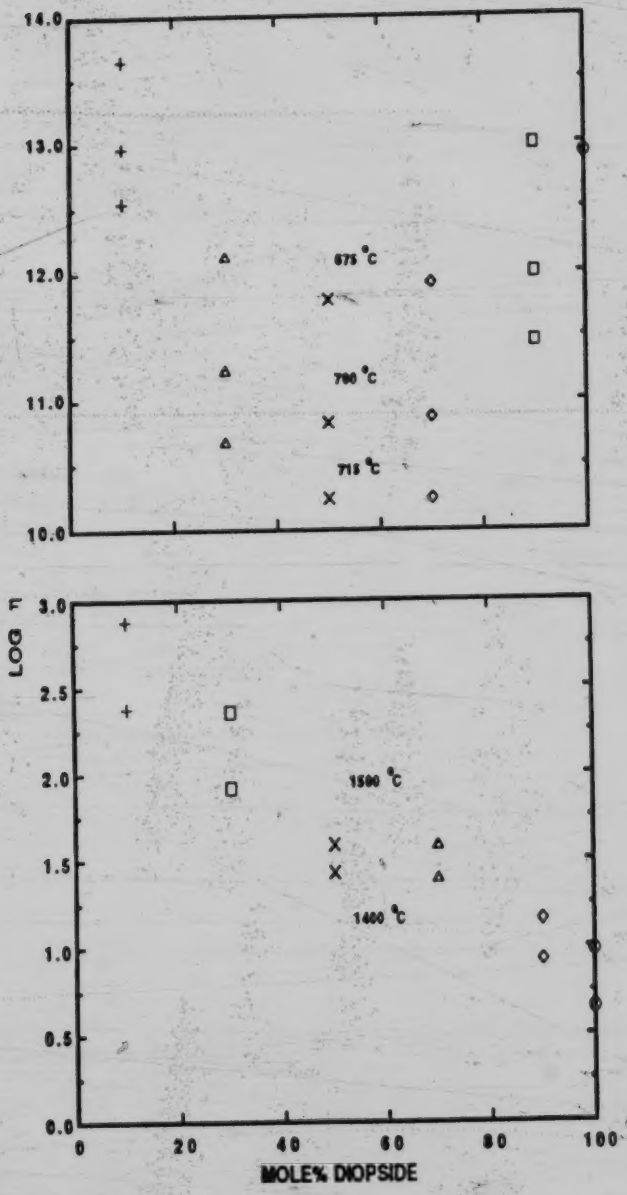

Figure 3.3 Log of the coefficient of viscosity (log η) vs. composition at several isotherms.

3.6 REFERENCES

Adam, G. and Gibbs, J. (1965) On the temperature dependence of cooperative relaxation properties in glass-forming systems. J. Chem. Phys. **43**, 139-146.

Bockris, J. and Lowe, D. (1954) Viscosity and the structure of molten silicates. Royal Soc. Lond. Proc. A226, 423-435.

Bockris, J., Mackenzie, J. and Kitchener, J. (1955) Viscous flow in silica and binary liquid silicates. Faraday Soc. Trans. **51**, 1734-1748.

Cranmer, D. and Uhlmann, D. (1981a) Viscosity of liquid albite, a network former. J. Non-Cryst. Solids **45**, 283-288.

Cranmer, D. and Uhlmann, D. (1981b) Viscosities in the system albite-anorthite. J. Geophys. Res. **86**, 7951-7956.

Cukiermann, M. and Uhlmann, D. (1973) Viscosity of liquid anorthite. J. Geophys. Res. **78**, 4920-4924.

Dingwell, D. (1986) Viscosity-temperature relationships in the system $Na_2Si_2O_5$-$Na_4Al_2O_5$. Geochim. Cosmochim. Acta **50**, 1261-1265.

Fulcher, G. (1925) Analysis of recent measurements of the viscosity of glasses. Bull. Am. Ceram. Soc. **8**, 339-355.

Hagy, H. (1963) Experimental evaluation of beam-bending method of determining glass viscosities in the range 10^8 to 10^{15} poises. J. Amer. Ceram. Soc. **46**, 93-97.

Hummel, W. and Arndt, J. (1985) Variation of viscosity with temperature and composition in the plagioclase system. Cont. Min. Pet. **90**, 83-92.

Isard, J. (1969) The mixed alkali effect in glass. J. Non-Cryst. Solids **1**, 235-261.

Lacy, E. (1967) The newtonian flow of simple silicate melts at high temperature. Phys. Chem. Glasses **8**, 238-246.

McMillan, P. (1984) A Raman spectroscopic study of glasses in the system CaO-MgO-SiO_2. Am. Min. **69**, 645-659.

Mysen, B., Virgo, D. and Scarfe, C. (1980) Relations between the anionic structure and viscosity of silicate melts- a Raman spectroscopic study. Am. Min. **65**, 690-710.

Mysen, B., Virgo, D. and Seifert, F. (1982) The structure of silicate melts: implications for chemical and physical properties of natural magmas.

Rev. Geophys. Space Phys. **20**, 353-383.

Richet, P. (1984) Viscosity and configurational entropy of silicate melts. Geochim. Cosmochim. Acta **48**, 471-483.

Riebling, E. (1966) Structure of sodium aluminosilicate melts containing at least 50 mole% SiO_2 at 1500°C. J. Chem. Phys. **44**, 2857-2865.

Scarfe, C. and Cronin, D. (1986) Viscosity-temperature relationships of melts at 1 atm in the systen diopside-albite. Am. Min. **71**, 767-771.

Scarfe, C., Cronin, D., Wenzel, J. and Kauffman, D. (1983) Viscosity-temperature relationships at 1 atm in the system diopside-anorthite. Am. Min. **68**, 1083-1088.

Seddon, E. (1939) J. Soc. Glass Tech. **23**, 36.

Shartsis, L., Spinner, S. and Capps, W. (1952) Density, expansivity, and viscosity of molten alkali silicates. J. Amer. Ceram. Soc. **35**, 155-160.

Sykes, D. and Scarfe, C. (1990) Melt structure in the system nepheline-diopside. J. Geophys. Res. **95**, 15745-15749.

Tauber, P. and Arndt, J. (1986) Viscosity-temperature relationship of liquid diopside. Phys. Earth Planet. Int. **43**, 97-103.

Tauber, P. and Arndt, J. (1987) The relationship between viscosity and temperature in the system anorthite-diopside. Chem. Geol. **62**, 71-81.

Taylor, M. and Brown, G. (1979a) Structure of mineral glasses. I. The feldspar glasses $NaAlSi_3O_8$, $KAlSi_3O_8$, $CaAl_2Si_2O_8$. Geochim. Cosmochim. Acta **43**, 61-77.

Taylor, M. and Brown, G. (1979b) Structure of mineral glasses. II. The SiO_2-$NaAlSiO_4$ join. Geochim. Cosmochim. Acta **43**, 1467-1475.

Uhlmann, D. (1972) Viscous flow in glass-forming liquids. In Amorphous Materials, ed. by Douglas, R. and Ellis, B., Wiley Interscience, 205-214.

4. SPECTROSCOPIC INVESTIGATION OF ANHYDROUS AND HYDROUS $KAlSi_3O_8$ GLASSES QUENCHED FROM HIGH PRESSURE

4.1 INTRODUCTION

An understanding of the mechanisms of structural transformation in melts at high pressure is required because a significant proportion of all igneous processes occur at depth. Of particular interest has been the role of Al in silicate melts. At one atmosphere, Al is in tetrahedral coordination in most silicate melts, but increasing pressure may induce a transformation to octahedral coordination (Waff, 1975). An increase in the coordination of Al has been the preferred explanation invoked to account for changes in melt densities and viscosities (Kushiro, 1976, 1978) and liquidus phase relations (Boettcher et al., 1984). Spectroscopic studies of glasses quenched from pressures less than 4 GPa do not support this interpretation (Sharma et al., 1979; McMillan and Graham, 1980; Fleet et al., 1984; Hochella and Brown, 1985). Recently, Ohtani et al. (1985) presented evidence for six-coordinated Al in $NaAlSi_3O_8$ glasses quenched from 6 GPa and 8 GPa. The results of Stebbins and Sykes (1990) on the same composition glass quenched from 8 GPa and 10 GPa disagree; these authors found no evidence of six-coordinated Al.

Solubility mechanisms for water in aluminosilicate melts generally involve a disruption of the extended network and production of nonbridging oxygens (Burnham, 1975; McMillan et al., 1983; Mysen and Virgo, 1986a,b), although other interpretations exist (Kohn et al., 1989). The presence of nonbridging oxygens in hydrous aluminosilicate melts may facilitate a change in

the coordination of Al with pressure.

The present study reports the results from a ^{27}Al, ^{29}Si MAS NMR, Raman, and IR investigation of the structure of anhydrous and hydrous $KAlSi_3O_8$ glasses quenched from high pressure. This composition was chosen because the one atmosphere glass structure is well characterized and the hydrous composition was found to be quenchable up to 7 GPa. Results are compared to previous investigations of anhydrous and hydrous high pressure aluminosilicate glasses.

4.2 METHODS

Sample Synthesis

The one atmosphere $KAlSi_3O_8$ starting glass was synthesized from high-purity, spectroscopic-grade oxides and carbonates. Approximately 0.2 wt% Gd_2O_3 was added to the starting material of the hydrous runs to decrease ^{29}Si spin relaxation times. This oxide was not added to the starting material of the anhydrous runs for reasons discussed below.

High pressure experiments (>2 GPa) were performed using the USSA 2000 ton split-sphere multianvil press at the C.M. Scarfe Laboratory of Experimental Petrology at the University of Alberta. The pressure cell consists of an 18 mm-edged (18M) MgO octahedron, ZrO2 and MgO inner sleeves, MgO and pyrophyllite spacers, and a stepped LaCrO3 heater (Figure 4.1). All parts are fired at 1000°C for one hour, to remove water, prior to sample loading. Pressure is transmitted to the sample assembly by means of eight WC anvils with

the corners truncated and fitted with preformed pyrophyllite and teflon gaskets. Pressure was calibrated using the fayalite- γ-spinel (5.3 GPa, 1000°C; Yagi et al., 1987) and coesite-stishovite (9.2 GPa, 1000°C; Yagi and Akimoto, 1976) phase transitions. Samples were first brought to the desired run pressure, then heated via the sectioned $LaCrO_3$ heater. Temperatures were monitored by a W3Re-W26Re thermocouple in contact with the top of the capsule. The emf of the thermocouple was not corrected for the effect of pressure or shear. Temperature gradients are less than 20°C across the length of the capsule with this design (Kanzaki, 1987; Wei et al., 1990). Samples were quenched, isobarically, within one minute of reaching the run temperature by disconnecting power to the furnace. Short run durations were necessary to minimize contamination of the sample by the capsule material (see below).

The anhydrous $KAlSi_3O_8$ glasses were synthesized at 8 GPa, 2000°C and 10 GPa, 2200°C. Initial experiments in single capsules made from Re-foil resulted in the presence of a Re-oxide phase disseminated throughout the glass. This was probably the result of the relatively high ambient fO_2 of the sample assembly. Consequently, a double-capsule assembly was used in subsequent runs. The one-atmosphere glass powder was loaded into the inner Re-capsule (2.2 mm ID, 2.3 mm OD, 2.5 mm L) and sealed by folding the edges of the capsule end. The charge was then placed in an outer Re-capsule (2.6 mm ID, 2.7 mm OD, 4.0 mm L), packed in W-metal powder, and the outer capsule sealed. Tungsten was used to maintain a low fO_2 because the fO_2 of the W-WO_2 transition is below that of the Re-ReO_2 transition, and in case of leakage, W-metal powder does not adversely effect the emf of the W3Re-W26Re thermocouple.

Run products were optically clear glasses with minor (approximately

0.3%) discrete opaque Re-oxide inclusions along the edges of the capsule material. The high-pressure $NaAlSi_3O_8$ glasses of Stebbins and Sykes (1990) were synthesized under similar conditions but were red in color. The red color of their glasses is believed due to the reduction of Gd^{3+} to a lower valence state, because the high-pressure anhydrous $KAlSi_3O_8$ glasses (Gd_2O_3- and FeO-free) are colorless, except for similar amounts of Re-oxide inclusions along the capsule interface. Optical examination (400X) and the MAS NMR, Raman, and IR results confirm the absence of a quench-crystalline phase in all anhydrous and hydrous glasses.

The 2 GPa (1500°C) runs were performed in a 19.0 mm solid-media piston-cylinder apparatus (Boyd and England, 1960). Experiments were conducted in a talc/pyrex/alumina furnace assembly. The 'hot piston-out' technique was used with a -13% friction correction. Temperature was monitored using Pt-Pt13Rh thermocouples with no pressure correction on the emf output. Run durations of three hours were terminated by disconnecting power to the furnace.

Hydrous $KAlSi_3O_8$ samples (Table 4.1) were synthesized at 2 GPa. A pre-determined amount of triply distilled water was loaded into the base of an open-ended 5.0 mm OD Pt-capsule with a microsyringe. The amount was checked by weight. One hundred seventy-five milligrams of glass powder was then loaded into the capsule and the entire assembly weighed. The capsule was then crimped, wrapped in a wet kim-wipe, and triple welded. The sample assembly was then reweighed to ensure there was no significant weight-loss. A difference of 1.0 mg or less was deemed acceptable.

Run products were optically clear glasses in the form of thin

decompression plates. To confirm that the samples were hydrous, several of these (unpolished) plates from each run were checked by transmission FTIR Spectroscopy (Digilab FTS-40 spectrometer). Measured intensities of the 5200 cm^{-1} and 4500 cm^{-1} peaks show a reasonable correlation with sample thickness and relative water contents.

Sample K2520 was used as the starting material for the hydrous high-pressure runs (Tabble 4.1). Run conditions were similar to the multianvil experiments reported above, except that samples were loaded into Pt-capsules (2.6 mm ID, 2.7 mm OD, 3.5 mm L), sealed, and run at 5 GPa (1750°C) and 7 GPa (1850°C). Runs were terminated after three minutes by disconnecting power to the furnace. Run products were optically clear and crystal-free.

MAS NMR Spectroscopy

^{29}Si and ^{27}Al MAS NMR measurements were collected using a Bruker AM-400 spectrometer (9.4 Tesla field) at Arizona State University. Samples were loaded into Delrin single air-bearing rotors contained in a Bruker MAS probe. ^{29}Si spectra were generated from 1000 4.5 μs pulses with delay times of 30 seconds. ^{27}Al spectra were obtained from 10,000 1 μs pulses with a delay of 0.5 seconds between each pulse. The MAS NMR results for the anhydrous 8 GPa and 10 GPa samples were obtained using a Varian VXR400s spectrometer (9.4 Tesla field) at Stanford University. Samples were loaded into ZrO_2 rotors contained in a Doty Scientific, Inc. high-speed 5.0 mm probe. ^{27}Al spectra were obtained from 40,000 0.5 μs pulses with delay times of 0.2 seconds. The spectrometers were tuned to the 79.5 MHz and 104.2 MHz resonant freqencies of

^{29}Si and ^{27}Al, respectively, and calibrated using TMS and 1M $Al(H_2O)_6^{3+}$ standards.

Raman and IR Spectroscopy

The unpolarized Raman spectra were collected using an Instrument S.A. U-1000 micro-Raman spectrometer at Arizona State University. Glass chips were excited with the 514.5 nm line of a Coherent Innova 90-4 Ar^+ laser having a source power of approximately 16 mW at the sample. This relatively low power was used to minimize heating and possible relaxation effects in the samples. A Nechet 40X objective was used to focus the beam onto the sample. The spectrometer was calibrated using the 520 cm^{-1} peak of Si-metal. Spectra were collected at 2 cm^{-1} steps with count times of 10 sec/step and using slit widths of 200 μm (slit 1) and 250 μm (slits 2-4). The unpolarized spectra were compiled from up to 25 scans.

Transmission FTIR spectra of powdered samples contained in KBr pellets were obtained with a Digilab FTS-40 spectrometer fitted with a ceramic Globar source, Michelson interferometer, KBr beamsplitter and a DTGS detector. Spectra were compiled from 256 scans.

4.3 RESULTS

Anhydrous Glasses

The one atmosphere Raman spectrum (Figure 4.2) is similar to the

$KAlSi_3O_8$ glass spectra of McMillan et al. (1982) and Matson et al. (1986). The intense band at 480 cm^{-1} is attributed to a delocalized vibrational mode involving the symmetric stretch of bridged oxygens in T-O-T (T= Si,Al) linkages (Bates, 1972; Sharma et al., 1981). These T-O-T linkages form a fully polymerized random network composed predominately of six-membered rings of tetrahedra (Taylor and Brown, 1979). The tetrahedra are denoted as Q^4 sites because all oxygens are bridging oxygens (Murdoch et al., 1985).

A band in the 560-600 cm^{-1} region is present in all fully polymerized network structures. The assigment of this band to symmetric stretching modes in three-membered rings of Q^4 tetrahedra is consistent with theoretical and experimental observations (Galeener, 1982; Revesz and Walrafen, 1982; Galeener and Geissberger, 1983; Henderson et al., 1985; Sykes and Scarfe, 1990). The ^{27}Al and ^{29}Si MAS NMR results of Murdoch et al.(1985) and Oestrike et al.(1987) indicate that Al-avoidance is largely obeyed in fully polymerized aluminosilicates and do not support the assignment of this band by McMillan et al. (1982) to vibrational modes in Al-O-Al linkages. The frequency and intensity of the 560 cm^{-1} band depends on Al/(Al + Si) (Sharma et al., 1978; Virgo et al., 1980; Mysen et al., 1980a; McMillan et al., 1982; Seifert et al., 1982) consistent with partitioning of aluminate tetrahedra into the three-membered ring configurations. Indeed, the most stable Si-O-Al bond angle (130°) calculated by De Jong and Brown (1980) is the same as the optimum T-O-T bond angle in three-membered rings (Galeener, 1982).

The mid-frequency envelope near 775 cm^{-1} is attributed to motion of the tetrahedral cation within its oxygen cage (Laughlin and Joannopoulos, 1977; Galeener and Mikkelsen, 1981; Galeener and Geissberger, 1983).

Previous investigations on albite (McMillan et al., 1982; Seifert et al., 1982) and orthoclase (McMillan et al., 1982) glasses have interpreted the high-frequency envelope based on a statistical curve-fitting of the data to fixed-frequency Gaussian bandshapes. The reliability of this method can be questioned for several reasons. Firstly, the distribution of T-O-T bond angles about the mean T-O-T bond angle is not necessarily symmetrical (Matson and Sharma 1985). Indeed, a small proportion of three-membered rings, if present, would impose a non-symmetrical distribution. Secondly, the number of component bands deemed to give the best fit to the high-frequency envelope of albite glass were significantly different between the two studies. This emphasizes the radically different interpretations that can emerge based on the statistical deconvolution method chosen. Thirdly, features of the high-frequency envelope in the spectra of all fully polymerized aluminosilicates and their Ga and Ge analogues (Mysen et al., 1980; McMillan et al., 1982; Seifert et al., 1982; Sharma et al., 1982; Henderson et al., 1985; Matson and Sharma, 1985; Matson et al., 1986) can be simply described in terms of two component bands with frequencies and intensities dependent on the Al(Ga)/Si(Ge) of the glass. The low-frequency band involves primarily Si-O antisymmetric stretching motions in Si-O-Al linkages (Sharma et al., 1982; Matson and Sharma, 1985). The frequency and intensity of this band decrease and increase, respectively, with increasing Al/Si. The high-frequency band involves primarily Si-O antisymmetric stretching motions in Si-O-Si linkages (Sharma et al., 1982; Matson and Sharma, 1985). The frequency of this band, therefore, is less sensitive to Al/Si than the lower frequency component.

For the orthoclase composition glass used in this study, the high-

frequency envelope is composed of two bands at 1015 cm^{-1} and 1100 cm^{-1} resulting from antisymmetric stretching vibrations of Si-O bonds in Si-O-Al and Si-O-Si linkages, respectively.

There are no observable changes in the position of the peaks with increasing pressure in either the Raman or IR spectra (Figures 4.2 and 4.3). In the low-frequency region of the Raman spectra, increasing pressure is accompanied by an increase in the intensity and narrowing of the 480 cm^{-1} peak and the loss of the shoulder at 560 cm^{-1}, which becomes an unresolvable component in the tail of the 480 cm^{-1} peak. The increased intensity in the 560 cm^{-1} region of the 2 GPa IR spectrum (Figure 4.3) indicates there is an asymmetric component to the vibrational mode responsible for this band. In the high-frequency region, the intensity of the 1015 cm^{-1} peak decreases relative to the intensity of the 1100 cm^{-1} peak in the 8 GPa and 10 GPa spectra (Figure 4.2).

MAS NMR peak positions and linewidths for all samples are listed in Table 4.1 The ^{27}Al MAS NMR spectra of the anhydrous high-pressure glasses are shown in Figure 4.4. The peak maximum associated with Q^4 ^{27}Al resonance, which occurs at 53.4 ppm in the one atmosphere spectrum, does not shift position in the 8 GPa and 10 GPa samples. This chemical shift is approximately 7 ppm more shielded than the ^{27}Al resonance in crystalline K-rich feldspars (Yang et al., 1986; Phillips et al., 1989), and consistent with the chemical shift of 53.8 ppm at 11.7 Tesla reported by Oestrike et al. (1987) for one atmosphere $KAlSi_3O_8$ glass. The high-pressure spectra are broadened and lineshapes are distinctly asymmetric with more intensity towards smaller chemical shifts resulting from the development of a shoulder near 25 ppm. This shoulder has not

developed in the 2 GPa spectrum (Figure 4.5). Albite glasses quenched at high-pressure have similar lineshapes to the sanidine glasses shown here (Stebbins and Sykes, 1990). No evidence for six-coordinated Al, which would have chemical shifts near 0 ppm, was observed.

Hydrous Glasses

2 GPa Glasses. The Raman and IR spectra of the hydrous 2 GPa glasses (Figures 4.3 and 4.6) are similar to those reported for hydrous silica and sodium aluminosilicate glasses (Stoien and Walrafen, 1976; Mysen et al., 1980b; McMillan et al., 1983; Mysen and Virgo, 1986a,b). A peak near 900 cm^{-1} appears in the spectra of all hydrous glasses, similar to the 950 cm^{-1} and 900 cm^{-1} peaks in SiO_2-H_2O and $NaAlSi_3O_8$-H_2O, respectively. Stolen and Walrafen (1976) and McMillan et al. (1983) assigned these bands to Si-(OH) and/or Al-(OH) vibrational modes. Mysen et al. (1980a) contested this assignment based on the apparent lack of an isotope shift (H-D). However, Freund (1982) has noted that Si-(OH) and Al-(OH) frequency shifts associated with H-D isotopic substitution would be no more than 15-25 cm^{-1} and unresolvable given the poor resolution of Raman spectra of amorphous materials. Mysen and Virgo (1986a,b) adopted the Si-(OH) assignment of the 950 cm^{-1} peak, but attributed the 900 cm^{-1} peak to Si-nonbridging oxygen (NBO) vibrational modes.

For the present discussion, the 900 cm^{-1} peak is assigned to Q^3 Al-(OH) stretching motions as these vibrational modes occur in the 700-900 cm^{-1} region (Kolesova and Ryskin, 1959; Ryskin, 1974). Q^1 vibrational modes do

appear near 900 cm^{-1} (Lazarev, 1972); however, mass balance considerations would require significant changes in the topology of the high-frequency envelope due to contributions from Q^2 and Q^3 units. Difference spectra generated from the subtraction of the Raman spectrum of the hydrous 2 GPa glass from the spectrum of the anhydrous 2 GPa sample reveals only changes in the 900 cm-1 region of the high-frequency envelope (Figure 4.7). The spectra were normalized to the intensity of the 480 $cm^{-1}$and 1015 cm^{-1} peaks of the anhydrous 2 GPa spectrum during separate subtraction routines. The difference spectra generated from these separate normalization procedures were identical. Assignment of this peak to Si-NBO vibrational modes is not warranted.

The intensity of the 900 cm^{-1} peak relative to the intensity of the high-frequency envelope remains constant for all of the hydrous 2 GPa glasses (Figure 4.3). This is consistent with the suggestion of Silver et al. (1990) that the OH/H_2O ratio in hydrous $KAlSi_3O_8$ glasses increases as total H_2O increases from zero to ~ 2-4 wt% total H_2O, beyond which any further addition of water increases only the amount of molecular H_2O dissolved in the melt.

In the ^{27}Al MAS NMR spectra, the ^{27}Al resonance is deshielded in the hydrous 2 GPa glasses relative to the anhydrous 2 GPa sample (Table 4.1, Figure 4.5). The peak maximum appears at 54.3 ppm for the hydrous glasses compared to 53.4 ppm for the anhydrous glass. The hydrous glasses have a linewidth of 13.3 ppm, 3.3 ppm narrower than the anhydrous glass. Kohn et al. (1989) reported similar behavior for the ^{27}Al resonance in Ab-H_2O glasses. It is interesting to note that the changes in the character of the ^{27}Al resonance spectra appear to correlate with the changes in the behavior of the 900 cm^{-1} peak in the Raman and IR spectra (Figures 4.3 and 4.6), consistent with the assignment of

the 900 cm^{-1} peak to Al-(OH) stretching modes. As in the anhydrous glass, no peak attributable to Al^{VI} was observed.

The peak maximum for the ^{29}Si resonance appears at -98.3 ppm for sample K2520 and is deshielded 1.5 ppm in the highest water content glass K7520 (Figure 4.8). Linewidth is essentially constant for the hydrous glasses (Table 4.1).

5 GPa and 7 GPa Glasses. The Raman and IR spectra of these high pressure glasses with 2.5 wt% total H_2O are given in Figures 4.3 and 4.6. The intensity of the 900 cm^{-1} peak decreases with pressure; in the 7 GPa spectra, it appears only as a weak shoulder. The behavior of this peak is consistent with the observations of Stolper (1982) that OH/H_2O, at constant total water content, decreases with increasing pressure. The intensity of the 1015 cm^{-1} peak decreases relative to the 1100 cm^{-1} peak with increasing pressure.

The ^{27}Al resonance in the spectrum for the 5 GPa glass appears at 52.6 ppm compared to 54.3 ppm for the 2 GPa sample K2520 (Figure 4.9). Spectral noise precludes a precise determination of peak maximum in the 7 GPa sample. Linewidths are 2.0 ppm and 2.5 ppm larger for the 5 GPa and 7 GPa samples than in sample K2520, respectively.

4.4 DISCUSSION

Anhydrous Glasses

As pressure is increased, the distribution of T-O-T bond angles about the

mean bond angle is reduced leading to narrower peak widths at 480 cm^{-1} in the Raman spectra (Figure 4.2). This is consistent with the conclusions of earlier investigations on other network glasses (Sharma et al., 1979; McMillan and Graham, 1981; Fleet et al., 1984; Hochella and Brown, 1985; Hemley et al., 1986). The reduced variability in T-O-T bond angle distribution would limit the ability of the network to compensate for the presence of three-membered rings and results in a distortion of the tetrahedral sites associated with these configurations. This loss of symmetry reduces the symmetric component of the T-O-T vibration, which decreases the intensity of the 560 cm-1 band in the Raman spectra and results in the appearance of this band in the IR spectra. Because aluminate tetrahedra are preferentially partitioned into the three-membered rings, the increased distortion also effects the Si-O vibrational modes associated with Si-O-Al linkages, which decreases the intensity of the Raman 1015 cm^{-1} peak.

Because ^{27}Al nuclei have spin (I) > 1/2, spectral lineshape and linewidth suffer from second-order quadrupolar broadening not removed by spinning at the magic-angle. This distortion is described by the quadrupolar coupling constant (Cq) and arises from the interaction of the nuclear electric quadrupole moment of the central nucleus with the electric field gradient about the central nucleus (Akitt, 1983; Harris, 1986). Perturbation of the electronic geometry increases the electric field gradient and the magnitude of Cq and broadens the lineshape towards smaller chemical shifts. In the anhydrous glasses, increased distortion of the tetrahedral configurations with pressure may result in an increase in Cq and produce the broad shoulder centered near 25 ppm in the 8 GPa and 10 GPa spectra (Figure 4.4). The behavior of the 560 cm^{-1} band in the Raman and IR

spectra (Figures 4.2 and 4.3) is consistent with the distortion of the three-membered ring configurations being largely responsible for the quadrupolar linebroadening. The absence of the shoulder in the 2 GPa ^{27}Al resonance spectrum (Figure 4.5) indicates these sites, at this pressure, are not sufficiently distorted to increase Cq, but are significant to induce a loss of polarization (Figure 4.3) and weaken the Raman signal (Figure 4.2).

The shoulder centered near 25 ppm in the ^{27}Al MAS NMR spectra occurs in the region where five-coordinated Al is known to resonate (Dupree et al., 1985; Risbud et al., 1987). One method of distinguishing quadrupolar linebroadening from a true chemical shift is to generate spectra at different magnetic field strengths (B_0). Because there is an inverse relation between Cq and B_0 and chemical shifts are field independent, spectral features associated with second-order quadrupolar effects can be identified. The ^{27}Al MAS NMR spectra of high-pressure albite glasses of Stebbins and Sykes (1990) are very similar to the sanidine composition glasses presented here. Because the lineshapes of their 8 GPa sample generated at different magnetic field strengths (400 MHz and 500 MHz) were essentially identical, they proposed that the position of the shoulder near 20 ppm resulted from the formation of more highly-coordinated Al sites. However, the difference in magnetic field strength in their study may not have been sufficient to affect an observable change in Cq. Kinsey et al. (1985) note that linewidths decrease more so for tetrahedral Al than for higher-coordinated Al with increasing magnetic field strength. Thus, a significant difference in magnetic field strength would more effectively diminish the second-order quadrupolar effects associated with the Q^4 ^{27}Al resonance and enhance resolution of the higher-coordinated Al site resonances, if these sites

exist. Therefore, it is possible that the shoulder near 25 ppm could result from either distortion of the three-membered rings or from higher-coordinated Al. At present, the former is favored because it is consistent with the interpretation of the Raman spectra. A MAS NMR study at even higher magnetic field strength, however, would clarify the interpretation of this region.

Hydrous Glasses

Solution mechanisms for water generally invoke the interaction of dissolved H_2O with bridged oxygens, resulting in the disruption of the extended network structure and the formation of Q^3-(OH) site symmetries (Burnham, 1975; Mysen et al., 1980; McMillan et al., 1983). Kohn et al. (1989) dispute this interpretation and suggest that the solution of H_2O occurs by exchange of H^+ for Na^+ as the charge-balancing cation and the formation of Na(OH) complexes. The model presented below favors the formation of Q^3-(OH) and is consistent with the general conclusions of Mysen and Virgo (1986b).

As noted earlier for the anhydrous glasses, an increase in pressure results in a narrower distribution of T-O-T bond angles associated with the six-membered rings, and a distortion of the Q^4 tetrahedra contained in the smaller-ringed configurations. The distorted nature of the three-membered rings make them relatively unstable with respect to other configurations in the network structure. Dissolution studies of mineral-fluid systems clearly indicate that high-energy defect sites are most susceptible to attack from dissolved volatile components (Berner, 1981). Thus, interaction of the high-energy three-membered ring configurations with H_2O may provide a mechanism for the

solution of H_2O in $KAlSi_3O_8$ melt. Depolymerization of the Q^4 aluminate tetrahedra in these smaller rings may be largely responsible for the formation of the Q^3 Al-(OH) sites because of their larger, charge-deficient tetrahedral cation, and would be consistent with the observed changes in the ^{27}Al resonance.

Kohn et al. (1989) discounted the presence of Q^3-(OH) species because Q^3 Al sites in layer silicates resonate around 70 ppm (Kinsey et al., 1985). However, it must be noted that the data of Kinsey et al. (1985) are for crystalline layer silicates, not glasses. The Q^4 ^{27}Al resonance in crystalline albite is deshielded by approximately 10 ppm from the Q^4 ^{27}Al resonance in the isochemical glass (Kohn et al., 1989). A similar separation would be expected for Q^3 Al sites. In addition, the nonbridging oxygens in the Q^3 Al sites of Kinsey et al. (1985) were bonded to octahedrally coordinated Mg and Al cations. This type of bond linkage is distinctly different in character from a terminal Q^3-(OH), making the analogy even more tenuous. The shorter Al-(OH) bond would result in a greater shielding of the central nucleus relative to a Q^3 linked to an octahedral Mg or Al, which would result in a smaller chemical shift. For comparison, the Si Q^3-(OH) resonance in SiO_2-H_2O appears at approximately -100 ppm (Maciel and Sindorf, 1980; Farnan et al., 1987), 11 ppm more shielded than the Si Q^3-ONa resonance in $Na_2Si_2O_5$ glass (Murdoch et al., 1985). Given the above considerations, the absence of a peak near 70 ppm does not preclude the existence of Q^3-(OH) sites, the resonance of which could be buried under the central peak associated with Q^4 Al resonance. Kohn et al. (1989) also noted that the increased electric field gradient of a Q^3 site would increase quadrupolar linebroadening. This, however, assumes that all Q^4 nuclei are in symmetrically well-defined sites. The NMR MAS, Raman and IR spectra are consistent with the interpretation

that some of the aluminate tetrahedra are associated with highly distorted three-membered ring configurations. The formation of a terminal Al-(OH) bond would partially decouple the ring complex from the extended network, reducing this distortion, and thereby, reducing quadrupolar linebroadening.

The proposed solution mechanism can be represented as follows

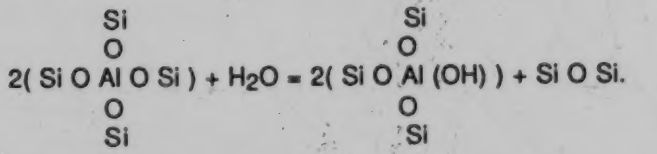

The formation of each Al-(OH) bond produces three Si Q^4 sites with one bridging oxygen connected to an Al Q^3 site. This would result in a slight deshielding of the central Si cation (Figure 4.8). The formation of Al-(OH) bonds also increase the number of Si-O-Si linkages. Normally, the wider distribution of ^{29}Si chemical environments would be reflected in increased ^{29}Si linewidths; however, the relatively small proportion of Si-O-Si linkages formed by this mechanism is probably below the resolution of the MAS NMR technique (<5%).

As pressure is increased, the OH/H_2O ratio decreases leading to reduced interaction with the aluminosilicate network. The fewer number of Q^3-(OH) sites results in a decrease in the intensity of the 900 cm^{-1} peak in the 5 GPa and 7 GPa Raman and IR spectra (Figures 4.3 and 4.6). The larger proportion of strained three-membered rings results in an increase in the distortion of the Si-O-Al linkages and weakens the intensity of the Raman signal at 1015 cm^{-1}. Similarly, the increased distortion broadens the ^{27}Al resonance linewidth (Figure 4.9).

4.5 CONCLUSION

The present results for the anhydrous glasses show no evidence for high-coordinated Al. The ^{27}Al MAS NMR spectra are very similar to the spectra of high pressure albite glass suggesting that the structures of these glasses behave in a consistent manner with increasing pressure. The effect of pressure on the structure of $KAlSi_3O_8$ glass is to reduce the distribution of T-O-T bond angles about the mean angle and to distort the three-membered ring configurations, at least to pressures up to 10 GPa. This distortion mainly effects the stretching vibrations associated with the aluminate tetrahedra.

The solution of H_2O is achieved by interaction of OH with the aluminate tetrahedra contained in the three-membered rings. Changes in the high-frequency envelopes in the Raman and IR spectra are not consistent with the formation of Si Q^3-(OH) sites.

Table 4.1 MAS NMR data for the anhydrous and hydrous $KAlSi_3O_8$ glasses quenched from .01 MPa (one atmosphere) and high-pressure.

	Pressure	wt% H_2O	^{27}Al peak max.	FWHM	^{29}Si peak max.	FWHM
K0001	.01 MPa	-	53.4 ppm	17.5 ppm	-	-
K0020	2 GPa	-	53.4 ppm	16.7 ppm	-	-
K2520	2 GPa	2.5	54.3 ppm	13.3 ppm	-98.3 ppm	16.7 ppm
K5020	2 GPa	5.0	54.3 ppm	13.3 ppm	-97.6 ppm	16.5 ppm
K7520	2 GPa	7.5	54.3 ppm	13.3 ppm	-96.8 ppm	16.3 ppm
K2550	5 GPa	2.5	52.6 ppm	15.3 ppm	-	-
K2570	7 GPa	2.5	55.1 ppm	15.8 ppm	-	-
K0080	8 GPa	-	53.0 ppm	-	-	-
K0100	10 GPa	-	53.0 ppm	-	-	-

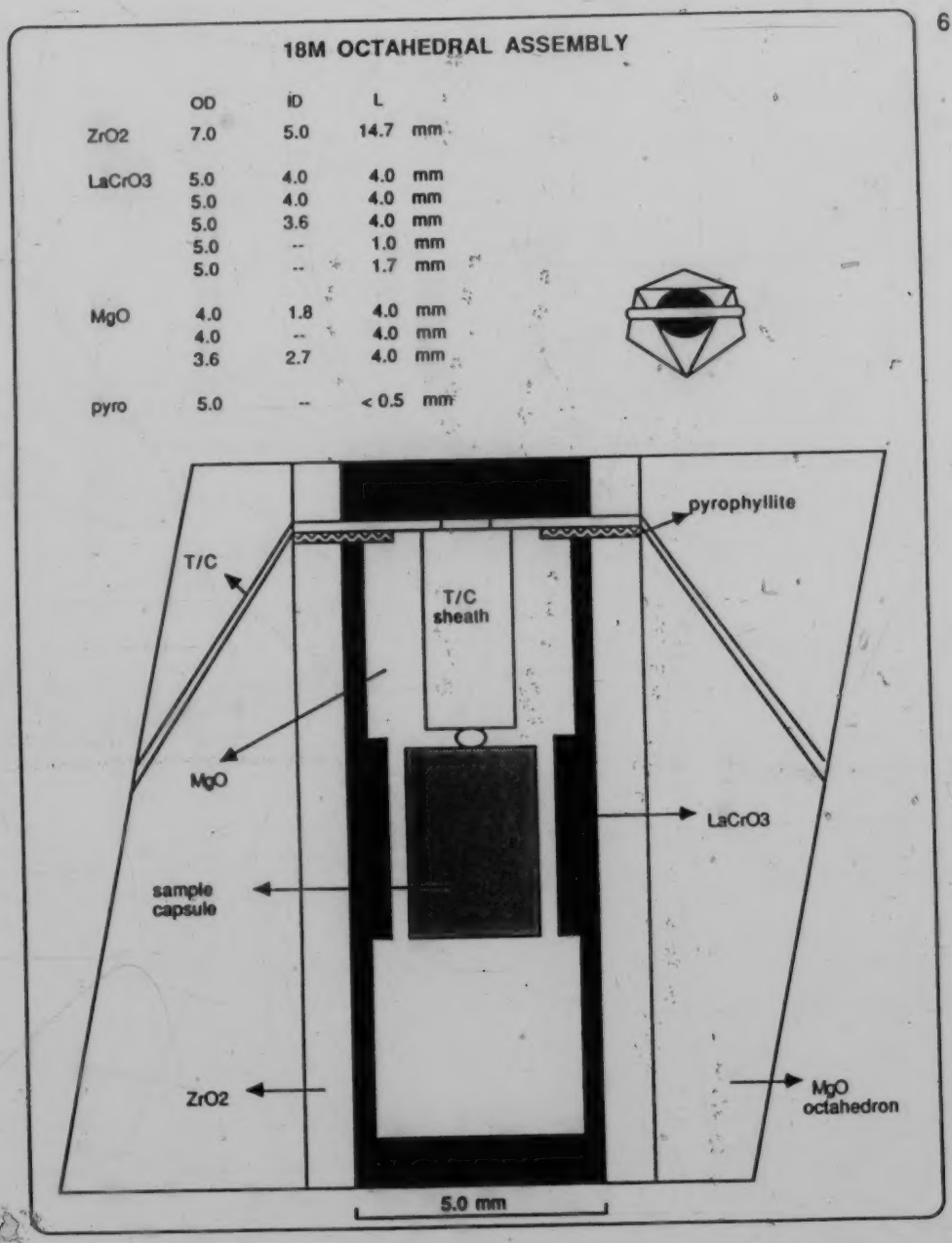

Figure 4.1 18M octahedral sample assembly used for high-pressure (> 2 GPa) sample synthesis. Sample is located in the central portion of the $LaCrO_3$ heater which is sectioned to minimize thermal gradients. Plan view is not to scale.

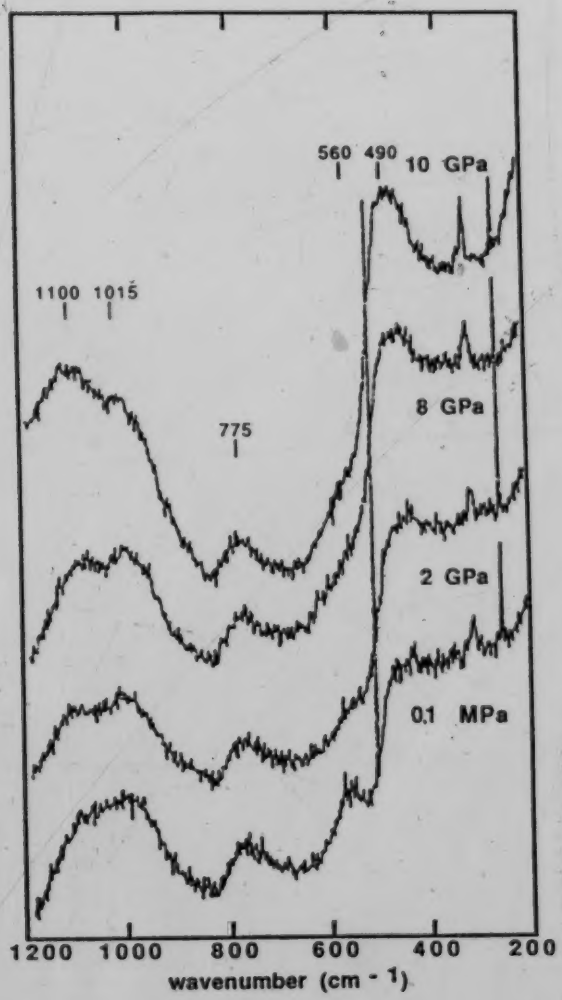

Figure 4.2 Unpolarized Raman spectra of anhydrous $KAlSi_3O_8$ glasses quenched from high pressure and the .01 MPa (one atmosphere) sample. The sharp spikes in the low frequency region are instrumental artefacts. Peak assignments are discussed in the text.

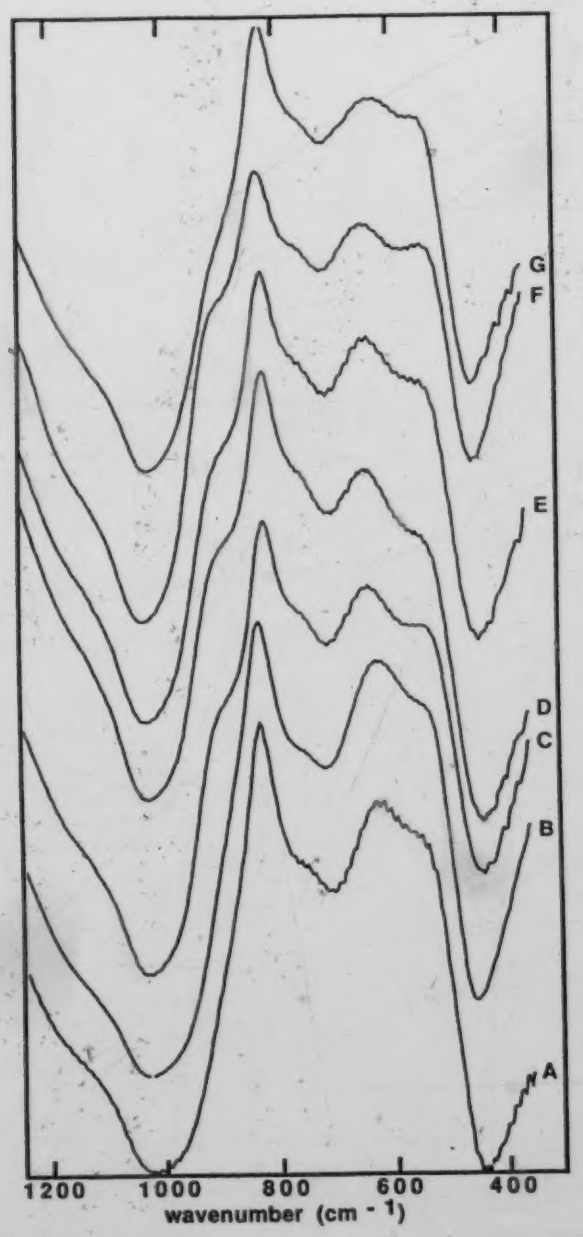

Figure 4.3 IR spectra of anhydrous and hydrous $KAlSi_3O_8$ glasses. A: 0.1 MPa (one atmosphere); B: 2 GPa, anhydrous; C: 2 GPa, 2.5 wt% H_2O; D: 2 GPa, 5.0 wt% H_2O; E: 2 GPa, 7.5 wt% H_2O; F: 5 GPa, 2.5 wt% H_2O; G: 7 GPa, 2.5 wt% H_2O.

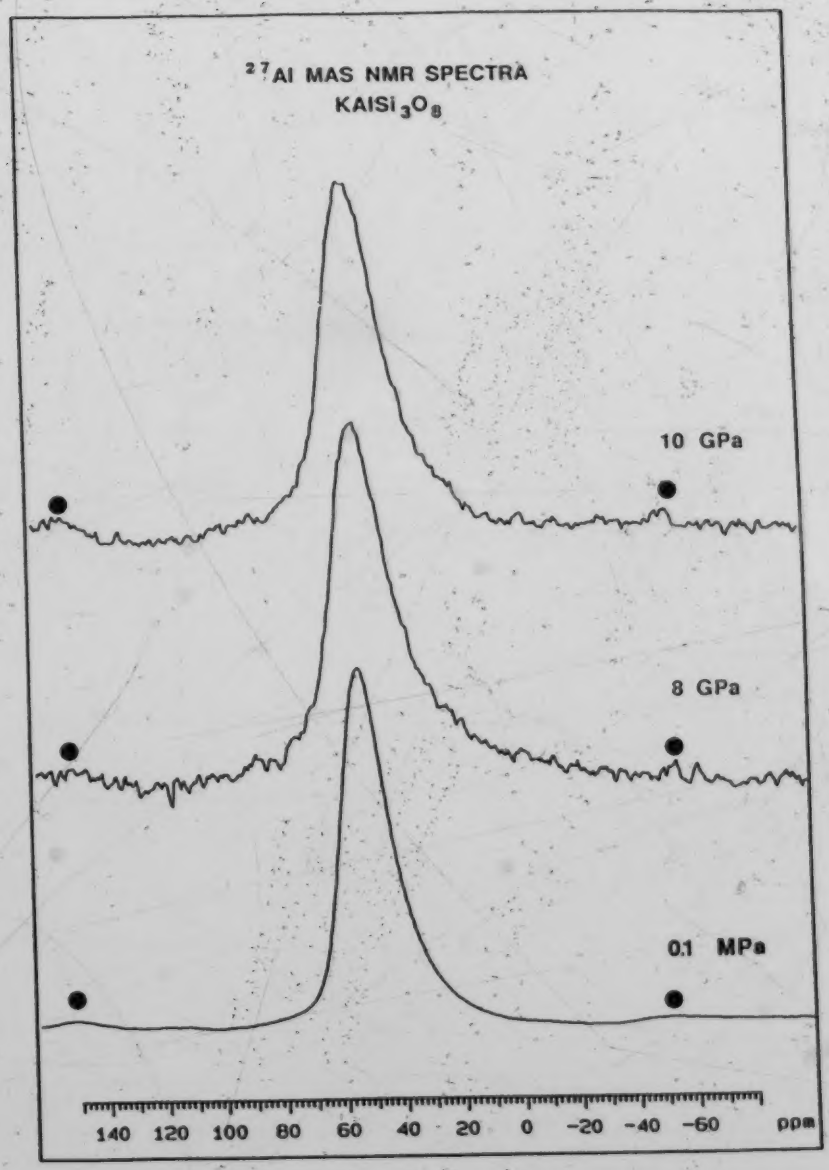

Figure 4.4 ^{27}Al MAS NMR spectra of the .01 MPa (one atmosphere), and 8 and 10 GPa glasses. A 100 Hz line broadening was applied during data processing. Frequency scale is relative to 1M aqueous $Al(NO_3)_3$. ● : spinning sidebands.

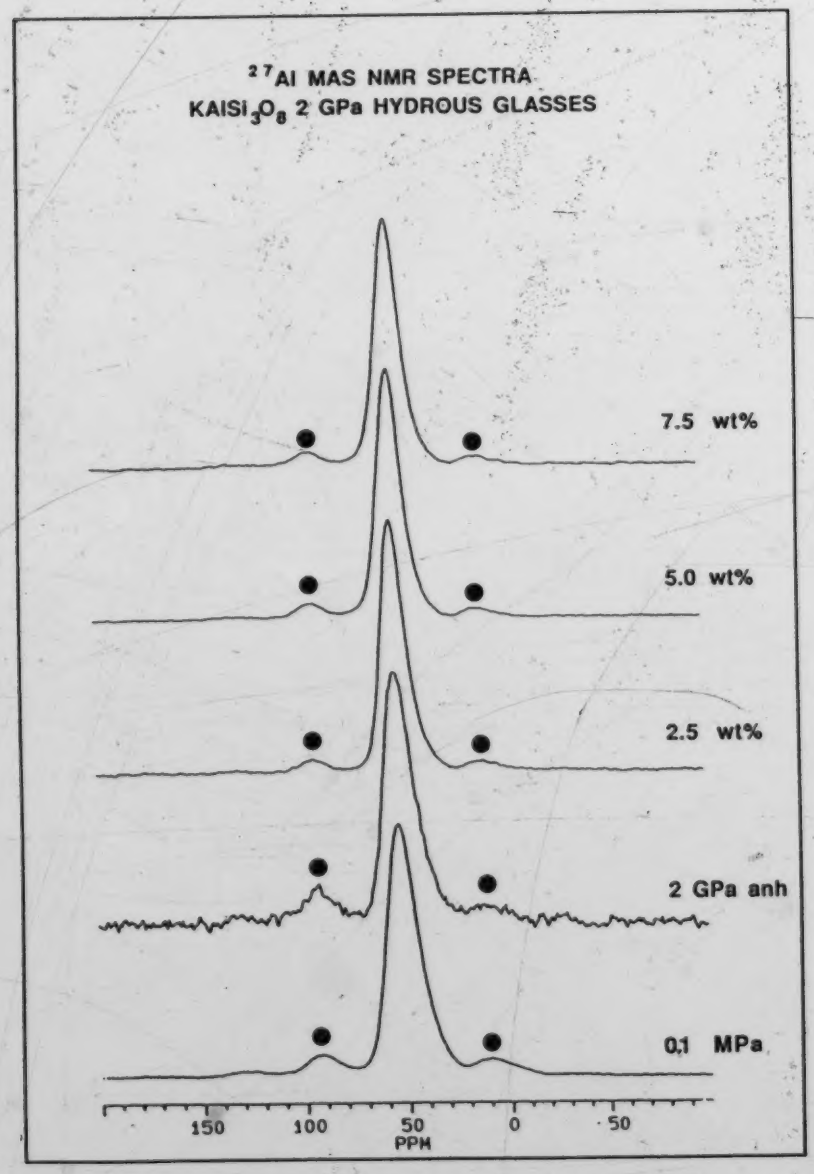

Figure 4.5 ^{27}Al MAS NMR spectra of hydrous $KAlSi_3O_8$ glasses quenched from 2 GPa. A 100 Hz line broadening was applied during data processing. Frequency scale is relative to 1M $Al(H_2O)_6^{3+}$. ● spinning sidebands.

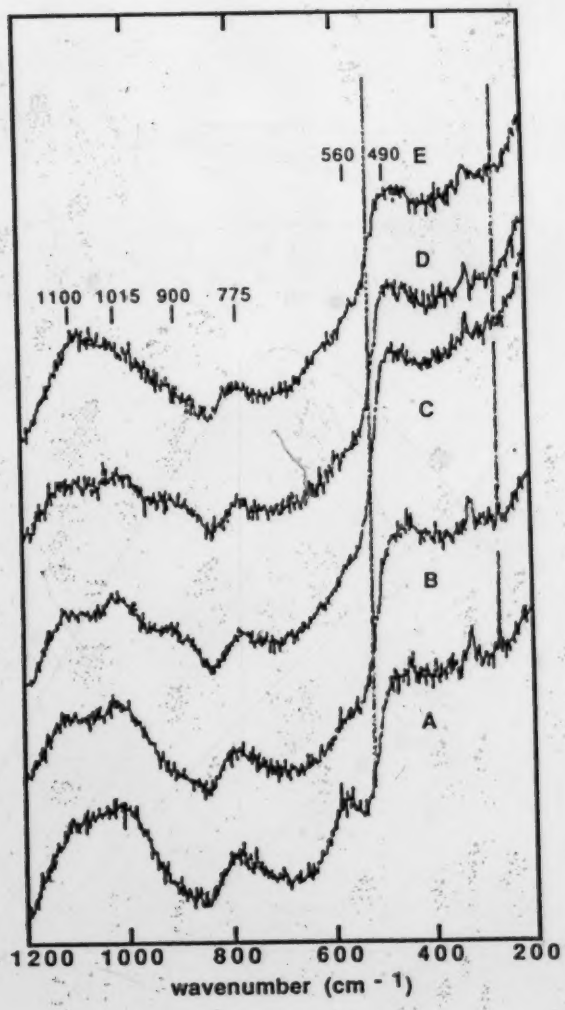

Figure 4.6 Unpolarized Raman spectra of anhydrous and hydrous $KAlSi_3O_8$ glasses. A: 0.1 MPa (one atmosphere); B: 2 GPa, anhydrous; C: 2 GPa, 5.0 wt% H_2O; D: 5 GPa, 2.5 wt% H_2O; E: 7 GPa, 2.5 wt% H_2O. The sharp spikes in the low frequency region are instrumental artefacts. Peak assignments are discussed in the text.

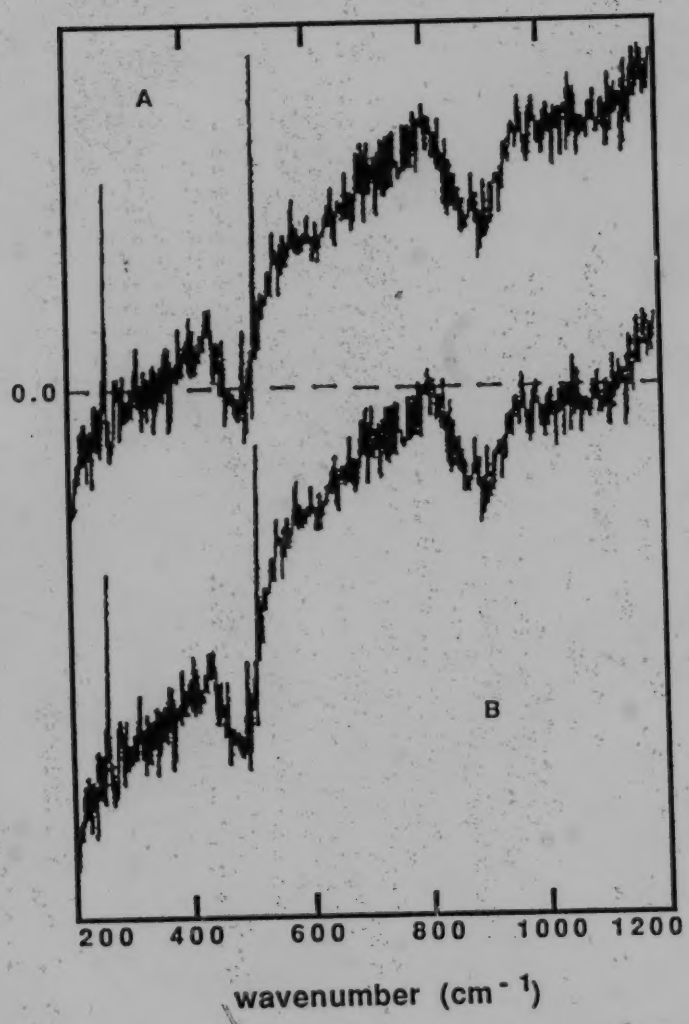

Figure 4.7 Raman difference spectra generated from subtraction of the 2 GPa, 5.0 wt% H2O spectrum from the 2 GPa anhydrous spectrum. A: normalized to the 480 cm-1 peak; B: normalized to the 1015 cm-1 peak.

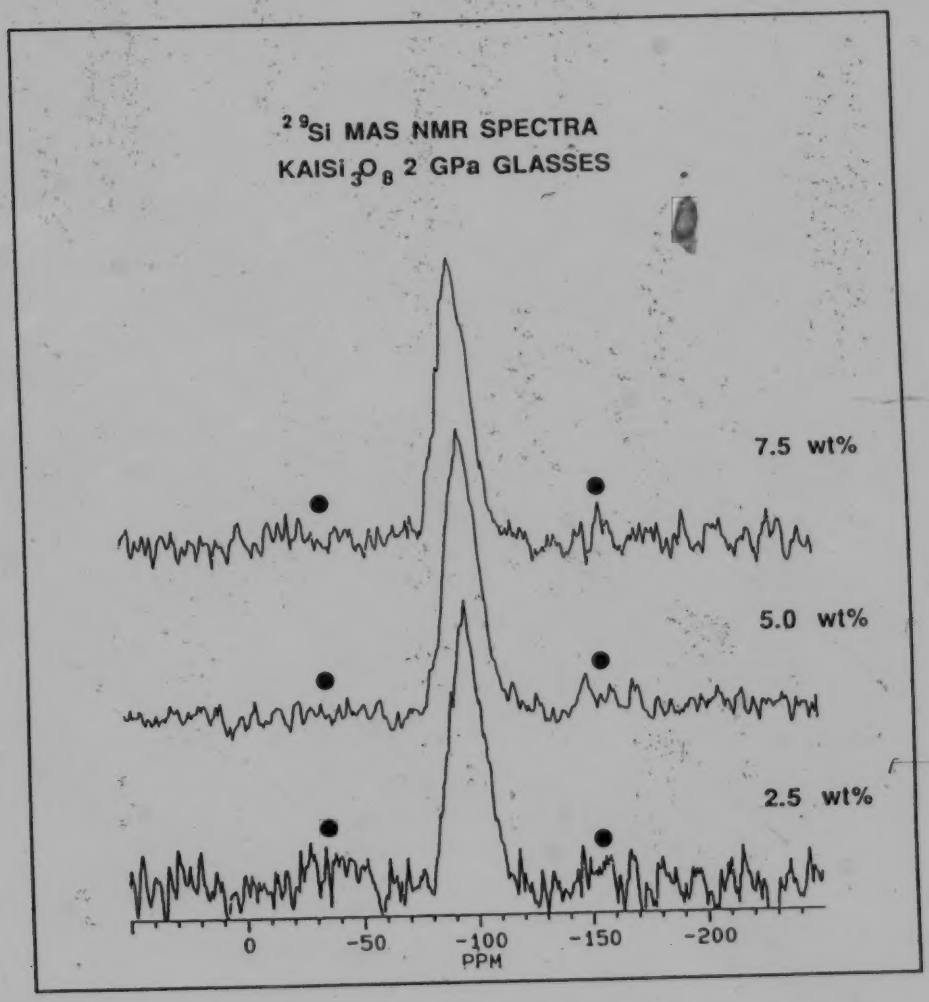

Figure 4.8 ^{29}Si MAS NMR spectra of hydrous $KAlSi_3O_8$ glasses quenched from 2 GPa. A 100 Hz line broadening was applied during data processing. Frequency scale is relative to TMS. ● : spinning sidebands.

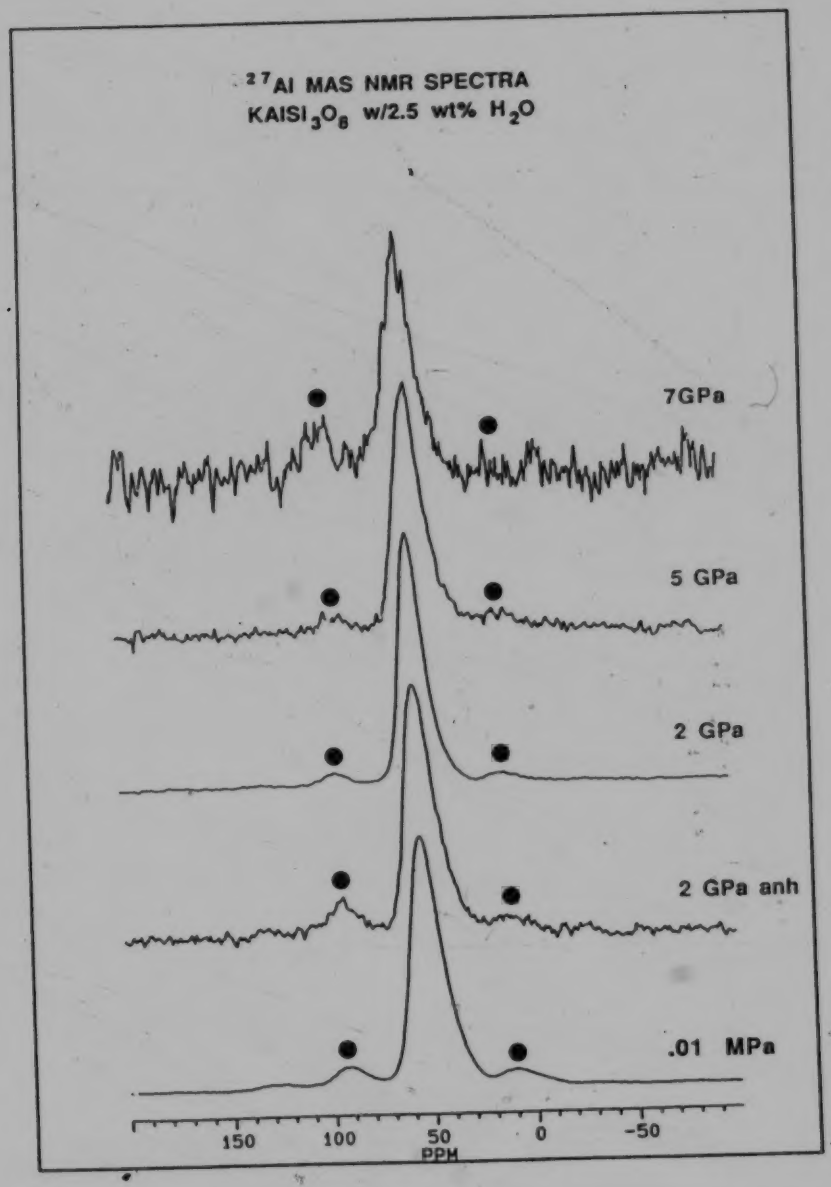

Figure 4.9 ^{27}Al MAS NMR spectra of hydrous $KAlSi_3O_8$ glasses with 2.5 wt% H_2O quenched from high pressure. A 100 Hz line broadening was applied during data processing. Frequency scale is relative to 1M $Al(H_2O)_6^{3+}$. ● spinning sidebands.

4.6 REFERENCES

Akitt, J. (1983) NMR and chemistry: an introduction to the fourier transform multinuclear era. Chapman and Hall, New York.

Bates, J. (1972) Dynamics of β-quartz structures of vitreous SiO_2 and BeF_2. J. Chem. Phys. **56**, 1910-1917.

Berner, R. (1981) Kinetics of weathering and diagenesis. In Kinetics of Geochemical Processes, ed. by Lasaga, A. and Kirkpatrick, R. Mineralogical Society of America, 111-134.

Boettcher, A., Guo, Q., Bohlen, S. and Hanson, B. (1984) Melting in feldspar-bearing systems to high pressures and the structures of aluminosilicate liquids. Geology **12**, 202-204.

Boyd, F. and England, J. (1960) Apparatus for phase-equilibrium measurements at pressures up to 50 kb and temperatures up to 1750°C. J. Geophys. Res. **65**, 741-748.

Burnham, C. (1975) Thermodynamics of melting in experimental silicate-volatile systems. Geochim Cosmochim. Acta **39**, 1077-1084.

Dupree, R., Farnan, I., Forty, A., El-Mashri., S. and Bottyan, L. (1985) A MAS NMR study of the structure of amorphous alumina films. J. Physique **46**, 113-117.

De Jong, B. and Brown, G. (1980) The polymerisation of silicate and aluminate tetrahadra in glasses, melts and aqueous systems- I. Electronic structure of $H_6Si_2O_7$, H_6AlSiO_7 and $H_6Al_2O_7$. Geochim. Cosmochim. Acta **44**, 491-511.

Farnan, I., Kohn, S. and Dupree, R. (1987) A study of the structural role of water in hydrous silica glass using cross-polarisation magic angle spinning NMR. Geochim. Cosmochim. Acta **51**, 2869-2874.

Fleet, M., Herzberg, C., Henderson, G., Crozier, E., Osborne, M. and Scarfe, C. (1984) Coordination of Fe, Ga and Ge in high pressure glasses by Mossbauer, Raman and X-ray absorption spectroscopy, and geological implications. Geochim. Cosmochim. Acta **48**, 1455-1466.

Freund, F. (1982) Solubility mechanisms of H_2O in silicate melts at high pressures and temperatures: a Raman spectroscopic study: discussion. Am. Min. **67**, 153-154.

Galeener, F. (1982) Planar rings in glasses. Solid State Comm. **44**, 1037-1040.

Galeener, F. and Geissberger, A. (1983) Vibrational dynamics in ^{30}Si-

substituted vitreous SiO_2. Phys. Rev. B **27**, 6199-6204.

Galeener, F. and Mikkelson, J. (1981) Vibrational dynamics in ^{18}O-substituted vitreous SiO_2. Phys. Rev. B **23**, 5527-5530.

Harris, R. (1986) Nuclear magnetic resonance spectroscopy. John Wiley and Sons, Inc., New York.

Hemley, R., Mao, H., Bell, P. and Mysen, B. (1986) Raman spectroscopy of SiO_2 glass at high pressure. Phys. Rev. Lett. **57**, 747-750.

Henderson, G., Bancroft, G., Fleet, M. and Rogers, D. (1985) Raman spectra of gallium and germanium substituted silicate glasses: variations in intermediate-range order. Am. Min. **70**, 946-960.

Hochella, M. and Brown, G. (1985) The structures of albite and jadeite composition glasses quenched from high pressure. Geochim. Cosmochim. Acta **49**, 1137-1142.

Kanzaki, M. (1987) Physical properties of silicate melts at high pressure. Ph.D. thesis, Geophysical Institute, University of Tokyo, Japan.

Kinsey, R., Kirkpatrick, R. Hower, J., Smith, K. and Oldfield, E. (1985) High resolution aluminum-27 and silicon-29 nuclear magnetic resonance spectroscopic study of layer silicates, including clay minerals. Am. Min. **70**, 537-548.

Kohn, S., Dupree, R. and Smith, M. (1989) A multinuclear magnetic resonance study of the structure of hydrous albite glasses. Geochim. Cosmochim. Acta **53**, 2925-2935.

Kolesova, V. and Ryslin, Y. (1959) Infrared absorption spectrum of hydrargillite $Al(OH)_3$. Optics Spec. **7**, 165-167.

Kushiro, I. (1978) Viscosity and structural changes of albite ($NaAlSi_3O_8$) melt at high pressures. Earth Planet. Sci. Lett. **41**, 87-90.

Kushiro, I. (1976) Changes in viscosity and structure of melt of $NaAlSi_2O_6$ composition at high pressures. J. Geophys. Res. **81**, 6347-6350.

Laughlin, R. and Joannopoulos, J. (1977) Phonons in amorphous silica. Phys. Rev. B **16**, 2942-2952.

Lazarev, A. (1972) Vibrational spectra and structure of silicates. Consultants Bureau, New York.

Maciel, G. and Sindorf, D. (1980) Silicon-29 nuclear magnetic resonance study of the surface of silica gel by cross-polarisation and magic-angle spinning. J. Amer. Chem. Soc. **102**, 7606-7607.

Matson, D., Sharma, S. and Philpotts, J. (1986) Raman spectra of some tectosilicates and of glasses along the orthoclase-anorthite and nepheline-anorthite joins. Am. Min. **71**, 694-704.

McMillan, P. and Graham, C. (1981) The Raman spectra of quenched albite and orthoclase glasses from 1 atm to 40 kb. In Progress in Experimental Petrology, ed. by Ford, C.,. NERC Publication Series D 18, 113-116.

McMillan, P., Jakobsson, S., Holloway, J. and Silver, L. (1983) A note on the Raman spectra of water-bearing albite glasses. Geochim. Cosmochim. Acta **47**, 1937-1943.

McMillan, P., Piriou, B. and Navrotsky, A. (1982) A Raman study of glasses along the joins silica-calcium aluminate, silica-sodium aluminate, and silica-potassium aluminate. Geochim. Cosmochim. Acta **46**, 2021-2037.

Murdoch, J., Stebbins, J. and Carmichael, I. (1985) High-resolution ^{29}Si NMR study of silicate and aluminosilicate glasses: the effect of network modifying cations. Am. Min. **70**, 332-343.

Mysen, B. and Virgo, D. (1986a) Volatiles in silicate melts at high pressure and temperature. 1. Interaction between OH groups and Si^{4+}, Al^{3+}, Ca^{2+}, Na^{+} and H^{+}. Chem. Geol. **57**, 303-331.

Mysen, B. and Virgo, D. (1986b) Volatiles in silicate melts at high pressure and temperature. 2. Water in melts along the join $NaAlO_2$-SiO_2 and a comparison of solubility mechanisms of water and fluorine. Chem. Geol. **57**, 333-358.

Mysen, B., Virgo, D. and Scarfe, C. (1980a) Relations between the anionic structure and viscosity of silicate melts- a Raman spectroscopic study. Am. Min. **65**, 690-710.

Mysen, B., Virgo, D., Harrison, W. and Scarfe, C. (1980b) Solubility mechanisms of H_2O in silicate melts at high pressures and temperatures: a Raman spectroscopic study. Am. Min. **65**, 900-914.

Oestrike, R., Yang, W-H., Kirkpatrick, R., Hervig, R. , Navrotsky, A. and Montez, B. (1987) High-resolution ^{23}Na, ^{27}Al, and ^{29}Si NMR spectroscopy of framework aluminosilicate glasses. Geochim. Cosmochim. Acta **51**, 2199-2210.

Ohtani, E., Taulelle, F. and Angell, C. (1985) Al^{3+} coordination changes in liquid aluminosilicates under pressure. Nature **314**, 78-81.

Phillips, B., Kirkpatrick, R. and Hovis, G. (1988) ^{27}Al, ^{29}Si, and ^{23}Na MAS NMR study of an Al,Si ordered alkali feldspar series. Phys. Chem. Min. **16**, 262-275.

Revesz, A. and Walrafen, G. (1983) Structural interpretations for some Raman lines from vitreous silica. J. Non-Cryst. Solids **54**, 323-333.

Risbud, S., Kirkpatrick, R., Taglialavore, A. and Montez, B. (1987) Solid-state NMR evidence of 4-, 5- and 6-fold aluminum sites in roller-quenched SiO_2-Al_2O_3 glasses. J. Am. Ceram. Soc. **70**, C10-C12.

Ryskin, Y. (1974) The vibrations of protons in minerals: hydroxyl, water and ammonium. In The Infrared Spectra of Minerals, ed. Farmer, V. Mineralogical Society, London, 137-181.

Seifert, F., Mysen, B. and Virgo, D. (1982) Three-dimensional network structure of quenched melts (glass) in the systems SiO_2-$NaAlO_2$, SiO_2-$CaAl_2O_4$ and SiO_2-$MgAl_2O_4$. Am. Min. **67**, 696-717.

Sharma, S., Smith, M. and Philpotts, J. (1982) Structures of glasses of plagioclase composition. **EOS** 63, p. 469.

Sharma, S., Mammone, J. and Nicol, M. (1981) Raman investigation of ring configurations in vitreous silica. Nature **292**, 140-141.

Sharma, S., Virgo, D. and Mysen, B. (1979) Raman study of the coordination of aluminum in jadeite melts as a function of pressure. Am. Min. **64**, 779-787.

Sharma, S., Virgo, D. and Mysen, B. (1978) Structure of melts along the join SiO_2-$NaAlSiO_4$ by Raman spectroscopy. CIWY **77**, 652-658.

Silver, L., Ihinger, P. and Stolper, E. (1990) The influence of bulk composition on the speciation of water in silicate glasses. Cont. Min. Pet. **104**, 142-162.

Stebbins, J. and Sykes, D. (1990) The structure of $NaAlSi_3O_8$ liquid at high-pressure: new constraints from NMR spectroscopy. Am. Min. **in press**.

Stolen, R. and Walrafen, G. (1976) Water and its relation to broken bond defects in fused silica. J. Chem. Phys. **64**, 2623-2631.

Stolper, E. (1982) Water in silicate glasses: an infrared spectroscopic study. Cont. Min. Pet. **81**, 1-17.

Taylor, M. and Brown, G. (1979) Structure of mineral glasses-II. The SiO_2-$NaAlSiO_4$ join. Geochim. Cosmochim. Acta **43**, 1467-1473.

Virgo, D., Mysen, B. and Kushiro, I. (1979) Anionic constitution of 1-atmosphere silicate melts: implications for the structure of igneous melts. Science **208**, 1371-1373.

Waff, H. (1975) Pressure-induced coordination changes in magmatic liquids. Geophys. Res. Lett. **3**, 193-196.

Wei, K., Tronnes, R. and Scarfe, C. (1990) Phase relations of aluminum-undepleted and aluminum-depleted komatiites at 4 GPa to 12 GPa. J. Geophys. Res., **in press**.

Yagi, T. and Akimoto, S. (1976) Direct determination of coesite-stishovite transition by in situ x-ray measurements. Tectonophysics **35**, 259-270.

Yagi, T., Akaogi, M., Shimomura, O., Suzuki, T. and Akimoto, S. (1987) In situ observation of the olivine-spinel phase transformation in Fe_2SiO_4 using synchrotron radiation. J. Geophys. Res. **92**, 6207-6213.

Yang, W-H., Kirkpatrick, R. and Henderson, D. (1986) High-resolution ^{29}Si, ^{27}Al, and ^{23}Na NMR spectroscopic study of Al-Si disordering in annealed albite and oligoclase. Am. Min. **71**, 712-726.

5. THESIS CONCLUSION and FINAL REMARKS

The three chapters that comprise the body of this thesis discuss the structure of silicate melts as a function of composition and pressure and its influence on the viscous properties of the melt phase.

CHAPTER 2

The Raman spectra of nepheline glass can be interpreted in terms of vibrational contributions from two distinct fully polymerized network structures, six- and three-membered rings of Q^4 tetrahedra. The aluminate tetrahedra appear to be preferentially partitioned into the available three-membered ring configurations. These results support the general conclusions of Seifert et al. (1982), although they favored the presence of two types of six-membered ring configurations. Stretching modes in Q^0, Q^1, Q^2 and Q^3 sites contribute to the vibrational spectra of diopside glass. The spectra of intermediate compositions (<18 mole% nepheline) can be described assuming contributions from only Q^2 and Q^4 tetrahedral sites. This tendency to develop molecular clusters results from the inability of Ca and Mg to compete with Na as the charge-balancing cation in structural units having only bridging oxygens (Q^4 units). This behavior was found by Dickinson and Scarfe (1990) in albite-diopside glasses and appears to be characteristic of diopside-sodium aluminosilicate systems.

If the mixing properties of network modifying cations have a significant influence on the structure of intermediate compositions, an investigation of the structure of melts in the systems $Na_2Si_2O_5$-$CaSi_2O_5$, $Na_2Si_2O_5$-$CaSiO_3$ and

Na_2SiO_3-$CaSi_2O_5$ would clarify the role of network modifying cations in systems where both endmembers are depolymerized. A hint as to the possible structural changes that might occur is the large immiscibility gap that appears in MO-SiO_2 systems but not in M_2O-SiO_2 systems. The formation of the immiscibility gap is consistent with the conclusions of the present investigation in that the alkali metal cations favor the more polymerized silicate structures and that the alkaline earth metals are associated with the more depolymerized units.

CHAPTER 3

High temperature melt viscosities in the system nepheline-diopside decrease with increasing diopside component and can be correlated to a decrease in the average size of the flow units. At low temperature, a viscosity minimum occurs at intermediate compositions and results from the greater temperature dependence of the viscosity of diopside melt relative to nepheline-rich compositions. The viscosity-composition-temperature relationships in nepheline-diopside g[illegible]s can be qualitatively described by the configurational entropy theory of cooperative relaxation processes (Adam and Gibbs, 1965; Richet, 1984). A more thorough quantitative test of the configurational entropy model requires the determination of heat capacity data for glassy and liquid nepheline.

The present results indicate that the most significant contributions to the temperature dependence of the configurational entropy term (and therefore viscosity) include the degree of polymerization of the endmembers and the type of ring configuration in fully polymerized network melts. It is difficult, as yet, to go beyond these observations because of the lack of low temperature viscosity and

heat capacity data and structural information for most silicate systems. However, an investigation of melt viscosities in the systems $Na_2Si_2O_5$-$CaSiO_3$, $CaSi_2O_5$-Na_2SiO_3 and $Na_2Si_2O_5$-Na_2SiO_3 may lend insight into other factors that may influence the temperature dependence of the size of the flow units (and therefore S_{conf} and viscosity). These factors include the type and distribution of Q^n sites, and the degree of mixing between nonframework cations.

CHAPTER 4

For anhydrous $KAlSi_3O_8$ glass, it was found that increasing pressure narrows the distribution of intertetrahedral angles about the mean angle which results in a distortion of the three-membered rings. High-coordinated Al was not observed for these glasses quenched from pressures up to 10 GPa. The question of whether coordination changes can be preserved on quenching (Williams and Jeanloz, 1988) requires in-situ high pressure-high temperature spectroscopic investigation. However, high-coordinated Al is quenchable at 1 bar (Risbud et al., 1987).

The solution of H_2O in high pressure $KAlSi_3O_8$ glasses is achieved by interaction of OH with the aluminate tetrahedra contained in the three-membered rings. The range of H_2O concentrations in the present study (25-55 mole%) correspond to an amount of OH that would require from 1/4 to 1/3 of all aluminum cations to be in tetrahedra associated with the three-membered ring configurations (Silver et al., 1990). While the present data cannot constrain the relative proportions of six- and three-membered ring configurations, the number of required three-membered rings appears high.

One of two possibilities can be invoked to amend the proposed solution

mechanism. First, the solution of water is achieved by interaction with all aluminate tetrahedra in six- and three-membered ring configurations. And second, after reaction with the distorted aluminate tetrahedra, H simply substitutes for K as the charge-balancing cation. This mechanism was originally proposed by Kohn et al. (1989) for hydrous albite glasses, although they suggested that this was the only water solubility mechanism.

Kohn et al. (1989) indicate that the major contribution to the ^{23}Na linewidth in hydrous albite (<30 mole% H_2O) is from a large chemical shift dispersion coupled with a weak contribution from second-order quadrupolar effects. At high water concentrations (>30 mole% H_2O), the relative contributions from chemical shift dispersion and quadrupolar effects to ^{23}Na linewidth are reversed. The ^{23}Na resonance systematics are in accord with the second alternative presented above.

Initially, OH groups react with the aluminate tetrahedra in the energetically-unfavorable three-membered rings to form Al Q^3-(OH) sites. The increased number of Al chemical environments (Q^4 and Q^3-(OH) sites) increases the chemical shift dispersion of the charge-balancing sodium cations (i.e. ^{23}Na nuclei also experience an increase in the number of chemical environments). Because Na maintains its charge-balancing role, the distribution of charge about the Na atom is not significantly altered, and therefore, does not lead to a significant increase in second-order quadrupolar effects.

At high water concentrations, the solution of water occurs by exchange of H for Na and no longer involves the aluminate tetrahedra. As the amount of water is increased, the proportion of Na atoms in NaOH complexes increase relative to the number occupying charge-balance sites. This leads to a decrease in the

chemical shift dispersion of the ^{23}Na resonance. However, the formation of NaOH complexes significantly alter the electronic charge distribution about the ^{23}Na atom and leads to significant second-order quadrupolar effects.

The most significant changes in the isotropic chemical shift and quadrupole coupling constant (Cq) for ^{23}Na occur at approximately 30 mole% H_2O (Kohn et al., 1989). The isotropic chemical shift is deshielded approximately 2 ppm from 0 to 30 mole% H_20, and by approximately 12 ppm between 30 to 60 mole% H_2O. The value of the quadrupole coupling constant remains constant up to 30 mole% H_2O, then increases dramatically for higher concentrations. It is possible that the change in the solution mechanism of H_2O, from interaction with the aluminate tetrahedra in the distorted three-membered rings to the exchange of H for Na, occurs at about 30 mole% water. This would be consistent with the observed inflections, at approximately 30 mole% total H_2O, in the wt% H_2O as dissolved OH vs. total wt% H_2O curves of Stolper (1982) and Silver et al. (1990) for aluminosilicate melt compositions, and in the log viscosity-molar OH/(OH + O) curve for hydrous albite melts (Dingwell, 1987).

Unfortunately, either the Kohn et al. (1989) model or the present model may be supported by the data. One potentially useful method to resolve this uncertainty is to synthesize an albite glass of composition $(H,Na)AlSi_3O_8$. If the present model is correct, the ^{27}Al resonance systematics for the above composition will differ significantly from the resonance spectra presented here.

5.1 REFERENCES

Adam, G. and Gibbs, J. (1965) On the temperature dependence of cooperative relaxation properties in glass-forming systems. J. Chem. Phys. **43**, 139-146.

Dickinson, J., Jr. and Scarfe, C. (1990) Raman spectroscopic study of glasses on the join diopside-albite. Geochim. Cosmochim. Acta **54**, 1037-1044.

Dingwell, D. (1987) Melt viscosities in the system $NaAlSi_3O_8$-H_2O-F_2O_{-1}. In Magmatic Processes: Physicochemical Principles, ed. by Mysen, B., Geochemical Society, 423-432.

Kohn, S., Dupree, R. and Smith, M. (1989) A multinuclear magnetic resonance study of the structure of hydrous albite glasses. Geochim. Cosmochim. Acta **53**, 2925-2935.

Richet, P. (1984) Viscosity and configurational entropy of silicate melts. Geochim. Cosmochim. Acta **48**, 471-483.

Risbud, S., Kirkpatrick, R., Taglialavore, A. and Montez, B. (1987) Solid-state NMR evidence of 4-, 5- and 6-fold aluminum sites in roller-quenched SiO_2-Al_2O_3 glasses. J. Amer. Ceram. Soc. **70**, C10-C12.

Seifert, F., Mysen, B. and Virgo, D. (1982) Three-dimensional network structure of quenched melts (glass) in the systems SiO_2-$NaAlO_2$, SiO_2-$CaAl_2O_4$ and SiO_2-$MgAl_2O_4$. Am. Min. **67**, 696-717.

Silver, L., Ihinger, P. and Stolper, E. (1990) The influence of bulk composition on the speciation of water in silicate glasses. Cont. Min. Pet. **104**, 142-162.

Stolper, E. (1982) Water in silicate glasses: an infrared spectrscopic study. Cont. Min. Pet. **81**, 1-17.

Williams, Q. and Jeanloz, R. (1988) Spectroscopic evidence for pressure-induced coordination changes in silicate glasses and melts. Science **239**, 902-905.